Investigation and Manipulation of Dislocations in Heteroepitaxial Diamond-on-Iridium Crystals

C. Stehl, M. Fischer, M. Schreck

Universität Augsburg, Institut für Physik, 86135 Augsburg, GERMANY

Outline

- Diamond for Radiation and Particle Detectors
- Growth of Heteroepitaxial Diamond Films on Ir/YSZ/Si(001)
- Defects in Crystals
- Dislocations in CVD Diamond
- Detection of Dislocations
- Reduction of Dislocation Density
- Further investigations

Diamond for Radiation and Particle Detectors

- **Influence of material quality on detector performance**

  Local variation of sensitivity
  → Electronic activity of crystal lattice defects and impurities (recombination centres)

X-ray response of a homoepitaxial single crystal diamond detector

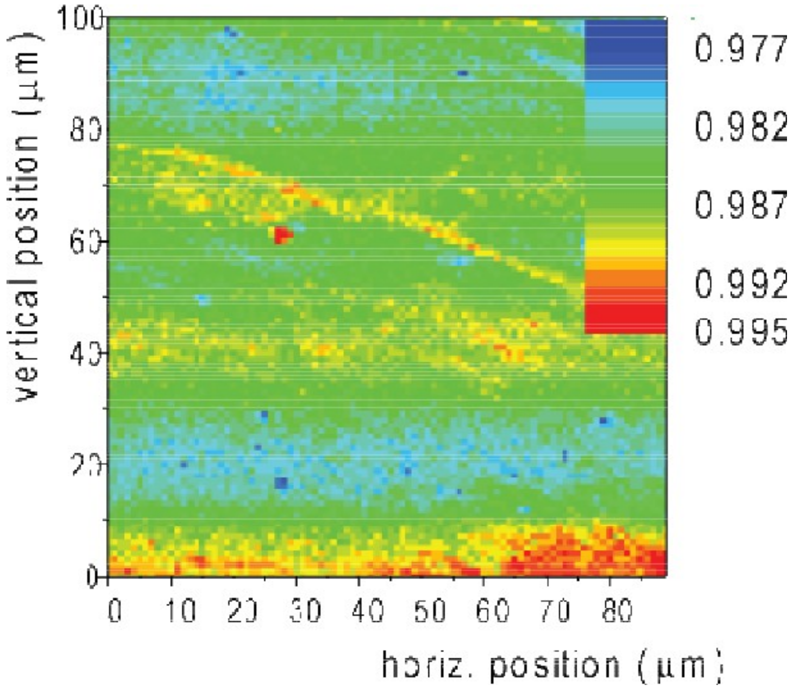

J. Morse, CARAT Workshop 2009

X-ray response of a polycrystalline diamond detector

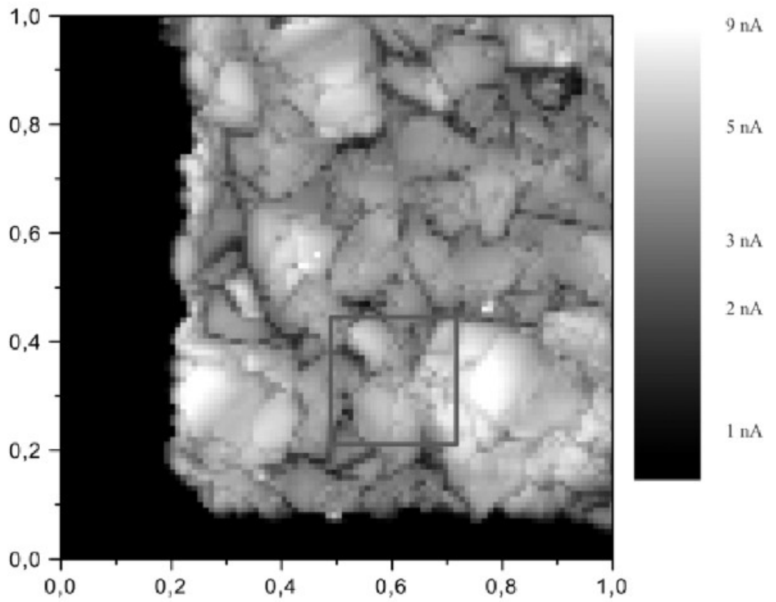

Fig. 3. Image of the X-ray sensitivity as measured on a 1= 1 mm area in the corner of the electrical contact. Grey scale is logarithmic and given in nA, for a 2.2= 10^8 ph $s^{y\ 1}$ flux at 5.5 keV.

P. Bergonzo et al., DRM 11 (2002), 418

Diamond for Radiation and Particle Detectors

- **Influence of material quality on detector performance**

  Local variation of sensitivity
  → Electronic activity of crystal lattice defects and impurities (recombination centres)

X-ray response of a homoepitaxial single crystal diamond detector

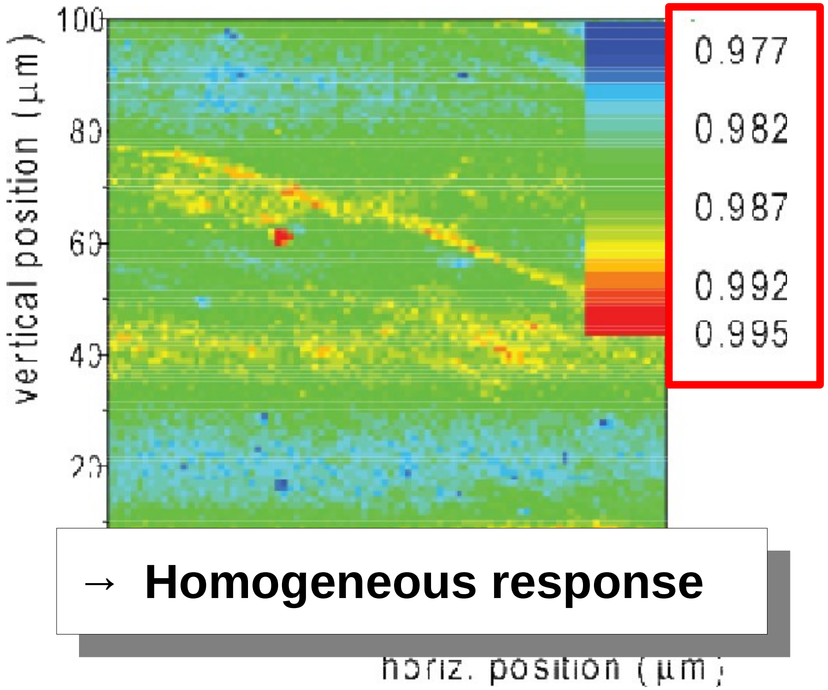

→ Homogeneous response

J. Morse, CARAT Workshop 2009

X-ray response of a polycrystalline diamond detector

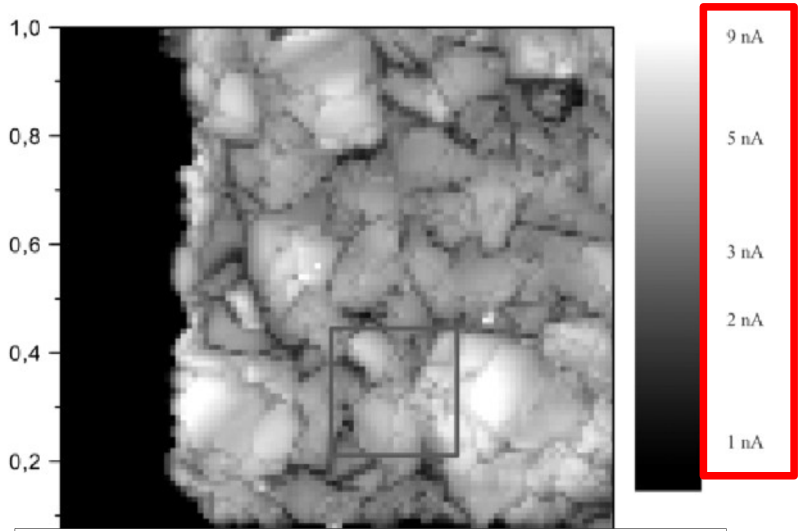

→ Inhomogeneous response

Fig. 3. Image of the X-ray sensitivity as measured on a 1× 1 mm area in the corner of the electrical contact. Grey scale is logarithmic and given in nA, for a 2.2× 10^8 ph s^{-1} flux at 5.5 keV.

P. Bergonzo et al., DRM 11 (2002), 418

Diamond for Radiation and Particle Detectors

- **Influence of material quality on detector performance**

  Local variation of sensitivity
  → Electronic activity of crystal lattice defects and impurities (recombination centres)

X-ray response of a homoepitaxial single crystal diamond detector

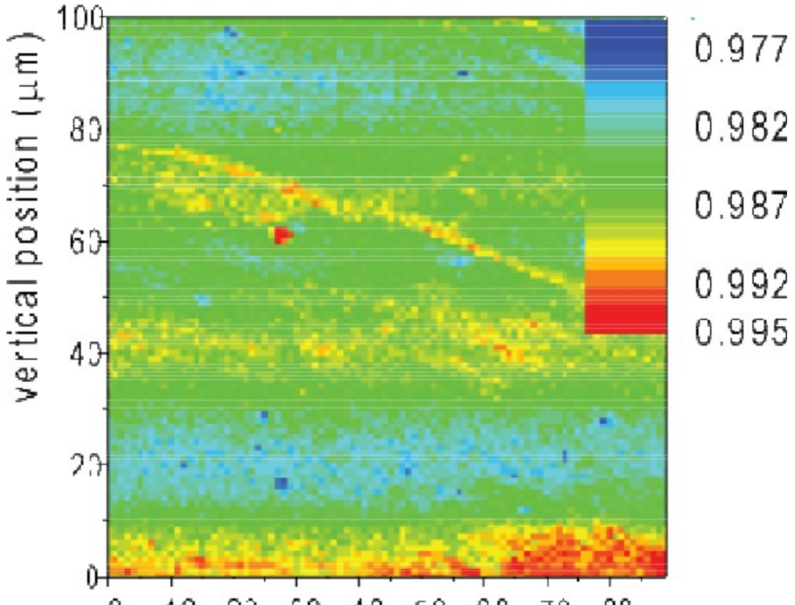

J. Morse, CARAT Workshop 2009

X-ray respnse of a polycrystalline diamond detector

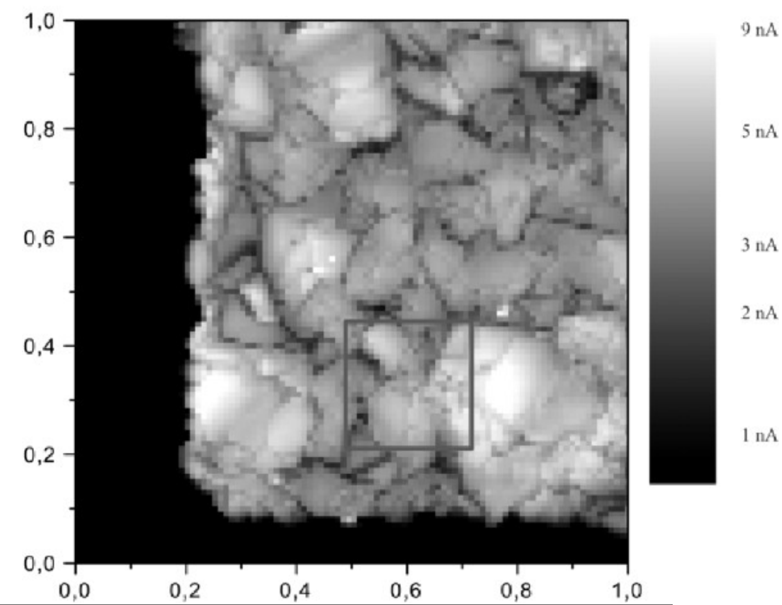

P. Bergonzo et al., DRM 11 (2002), 418

→ Possibilities for measuring and influencing the defect concentration?

- **Method of growth**

  Microwave enhanced plasma chemical vapour deposition (MWPCVD)

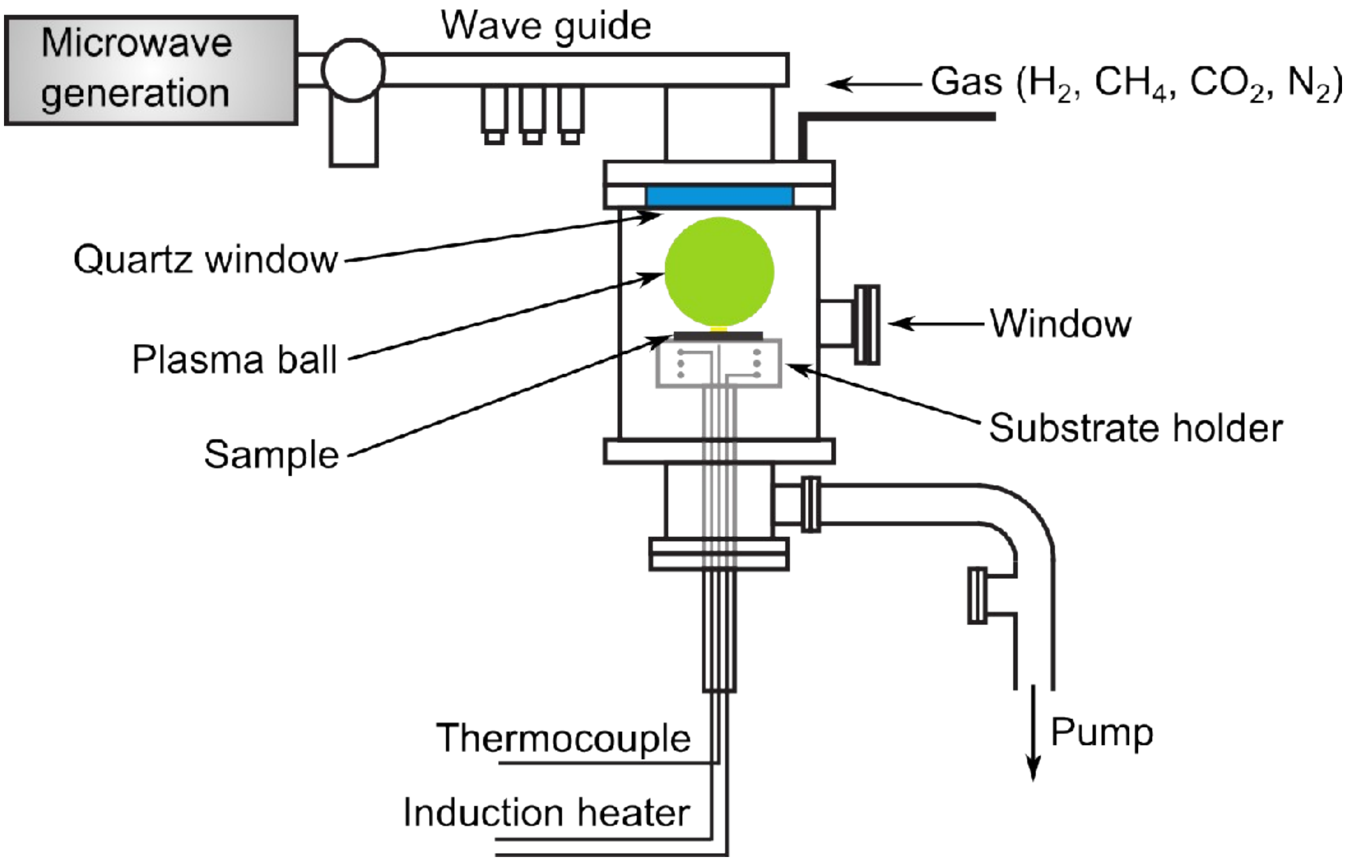

Schematic and photograph of CVD reactor

Heteroepitaxial Diamond Films on Ir/YSZ/Si(001)

- **Substrate**

  Multi-layer system Ir/YSZ/Si(001) (YSZ = yttria-stabilised zirconia)
  → Good thermal compatibility of diamond and silicon
  → Monocrystalline growth of diamond on iridium
  → Cost-saving (Ir price!) due to thin film technology

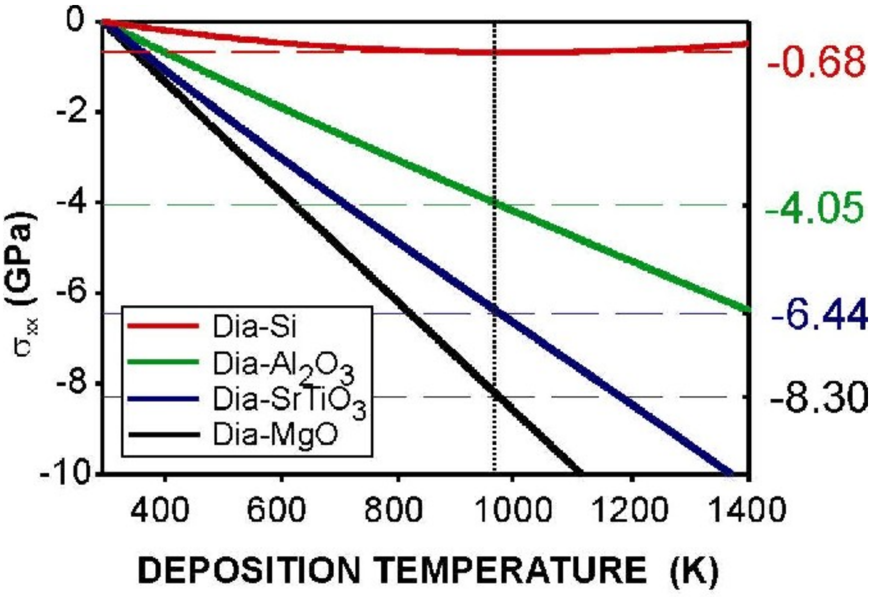

Thermally induced stress due to mismatched thermal expansion coefficients of diamond and substrate

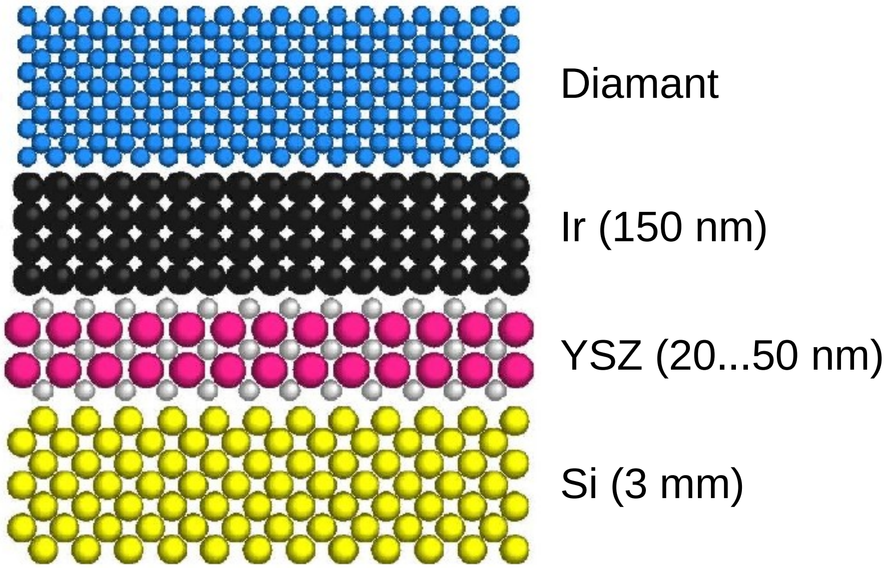

Schematic of diamond/Ir/YSZ/Si multi-layer system

Heteroepitaxial Diamond Films on Ir/YSZ/Si(001)

- **Nucleation**

  Bias-Enhanced Nucleation (BEN)
  → Applicable to 4 inch Ir/YSZ/Si(001) wafers
  → Nucleation density up to 10^{11} cm^{-2}

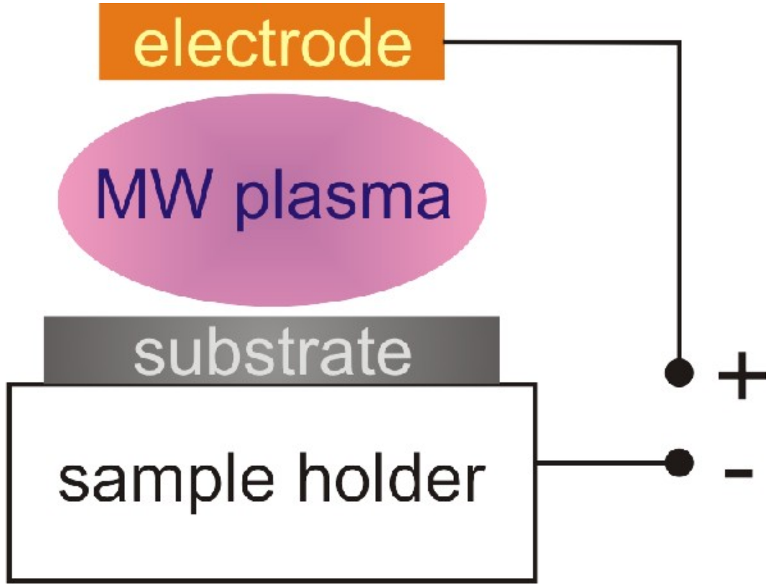

Schematic of BEN set-up

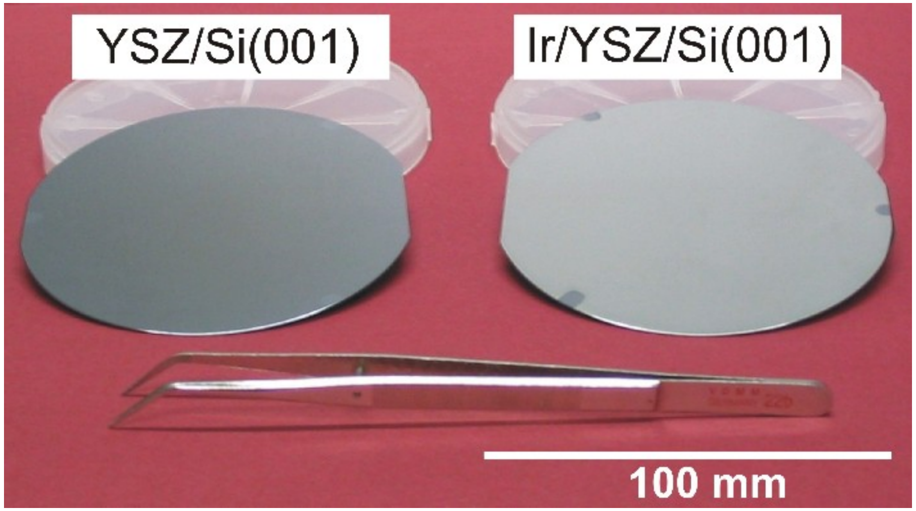

4 inch substrates for BEN process

- **Growth**

  → Formation of defect-rich monocrystalline diamond film
  → Improvement of crystalline quality with film thickness

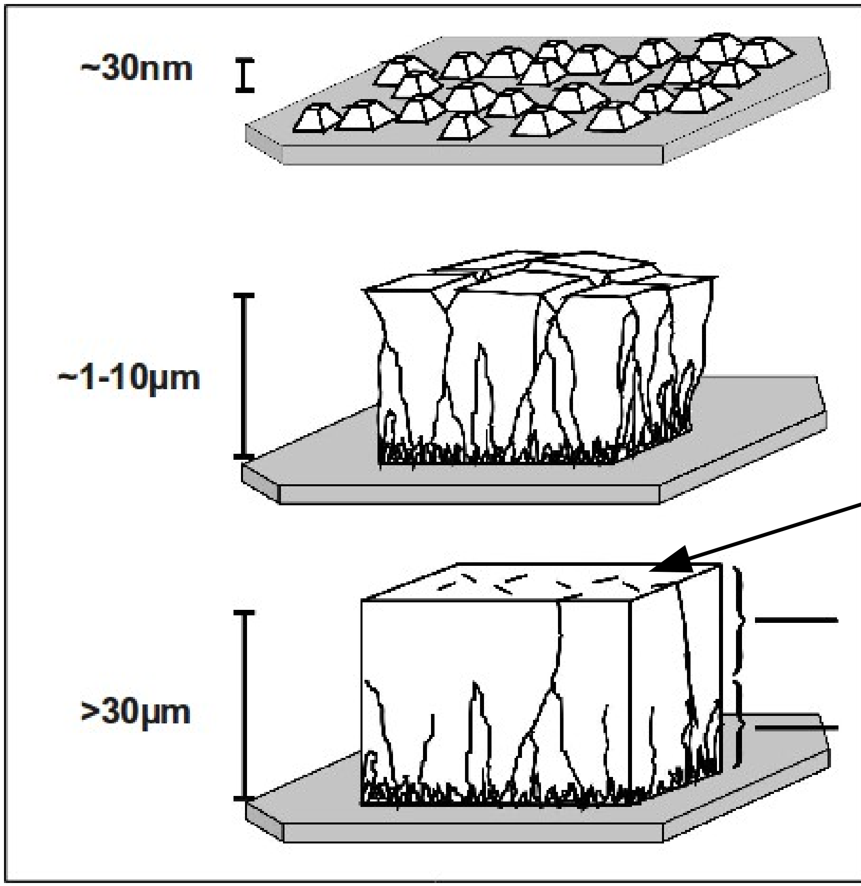

Schematic: Transition to heteroepitaxial diamond single crystal

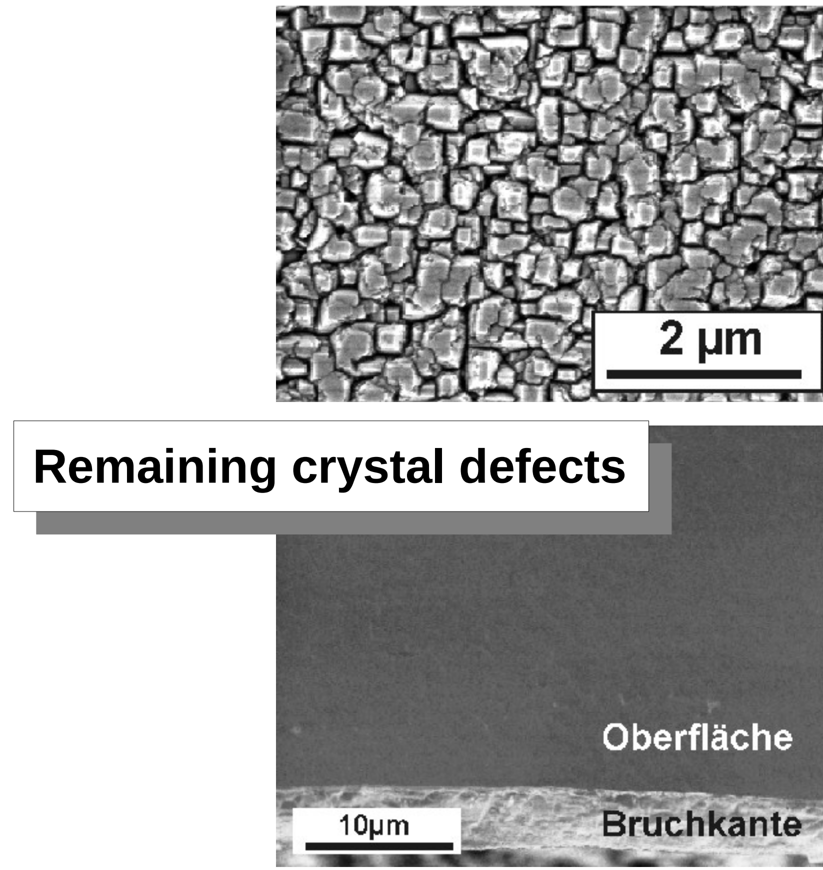

SEM images of Dia/Ir/$SrTiO_3$/Si(001)

Heteroepitaxial Diamond Films on Ir/YSZ/Si(001)

- **State of the art**
  Large-area growth
  → Step by step towards 30 x 30 mm²

10 x 10 mm² flawless detector crystal

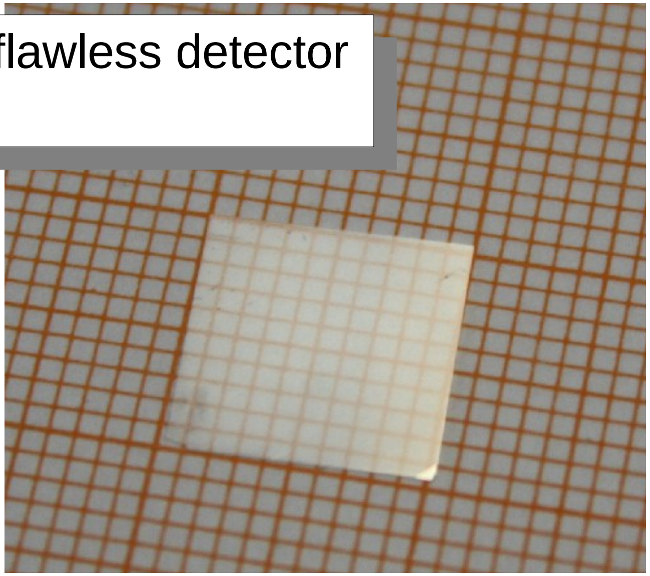

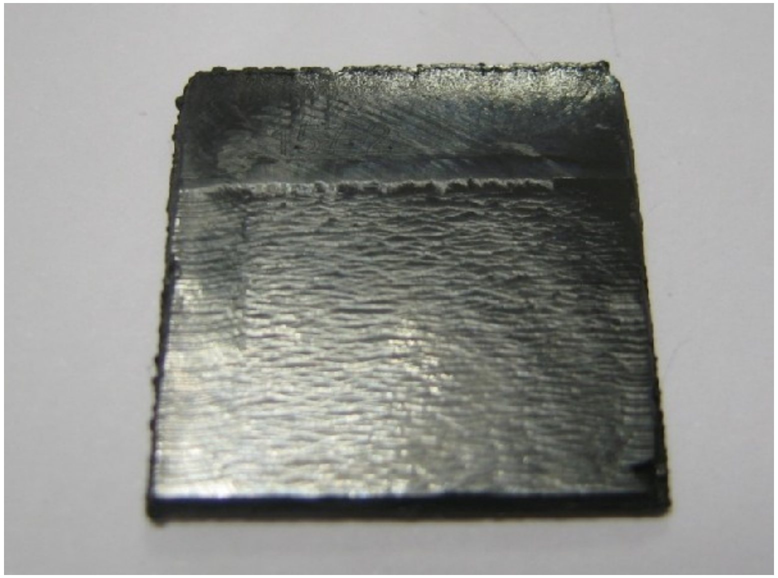

20 x 20 mm² neutron monochromator crystals (“poor” quality)

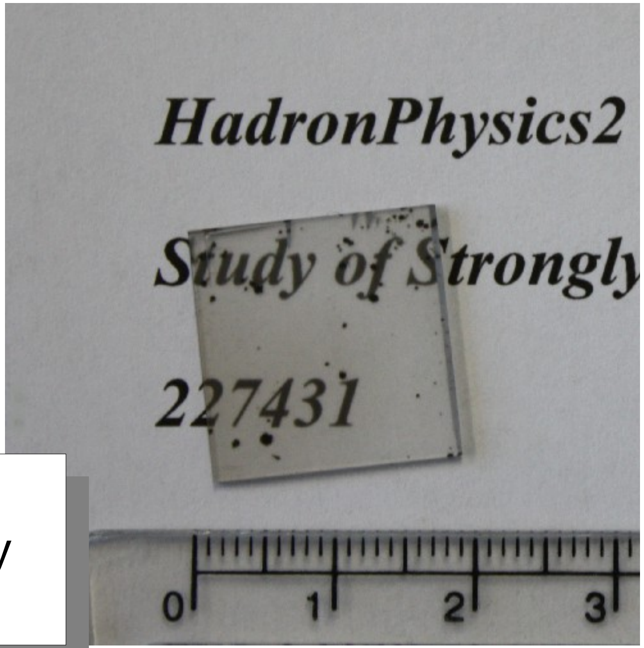

18 x 18 mm² attempt for detector crystal (medium quality, still many inclusions)

- **State of the art**
  Detector performance
  → Resolution of discrete mixed nuclide α particle energy spectrum

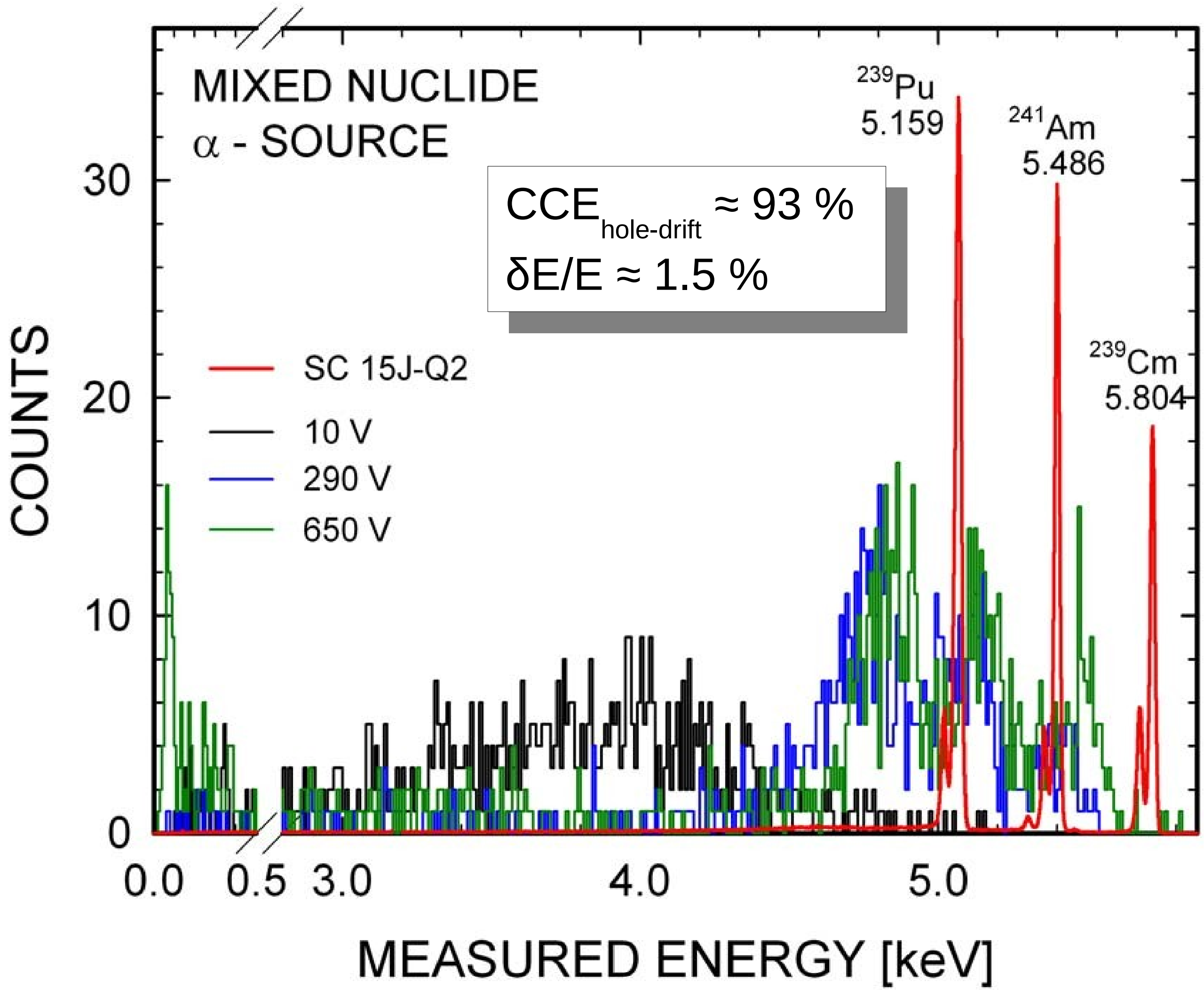

E. Berdermann, CARAT-Workshop 2011

Defects in Crystals

Point defects (0-dimensional)
e.g. vacancies and interstitials

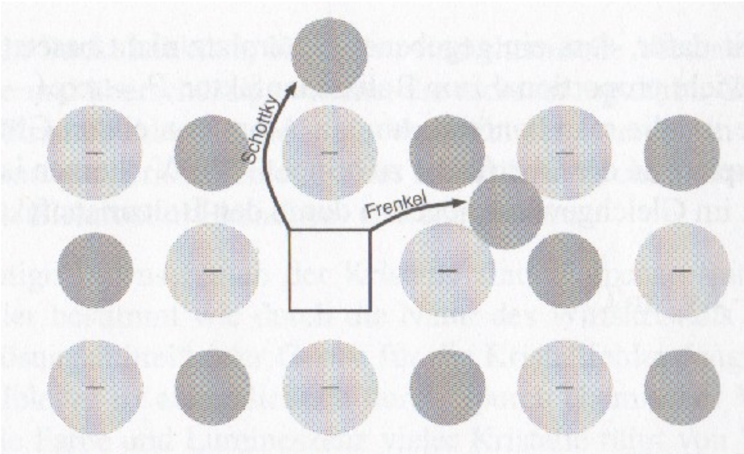

C. Kittel: Einführung in die Festkörperphysik, 14th ed. (2006)

Line defects (1-dimensional)
e.g. dislocations

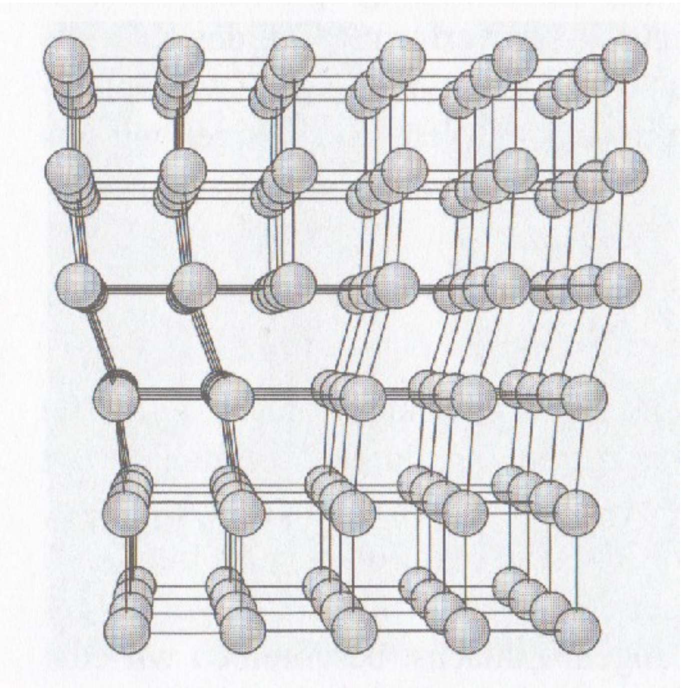

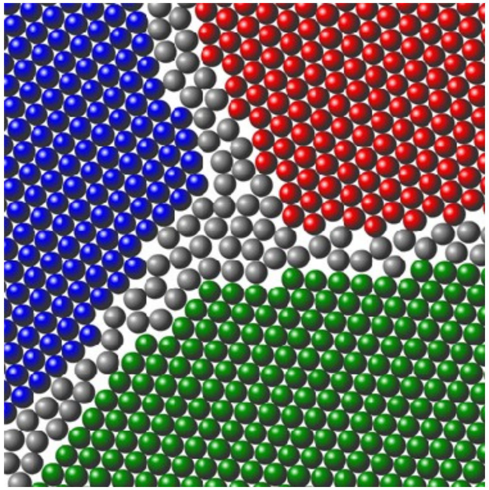

Planar defects (2-dimensional)
e.g. grain boundaries

http://www.spaceflight.esa.int/impress/text/education/Glossary/Glossary_G.html

Bulk defects (3-dimensional)
e.g. voids (= clusters of vacancies)

Dislocations in CVD Diamond

- **Basics**

  Fundamental dislocation types

Insertion of additional incomplete lattice plane

Edge dislocation

Screw dislocation

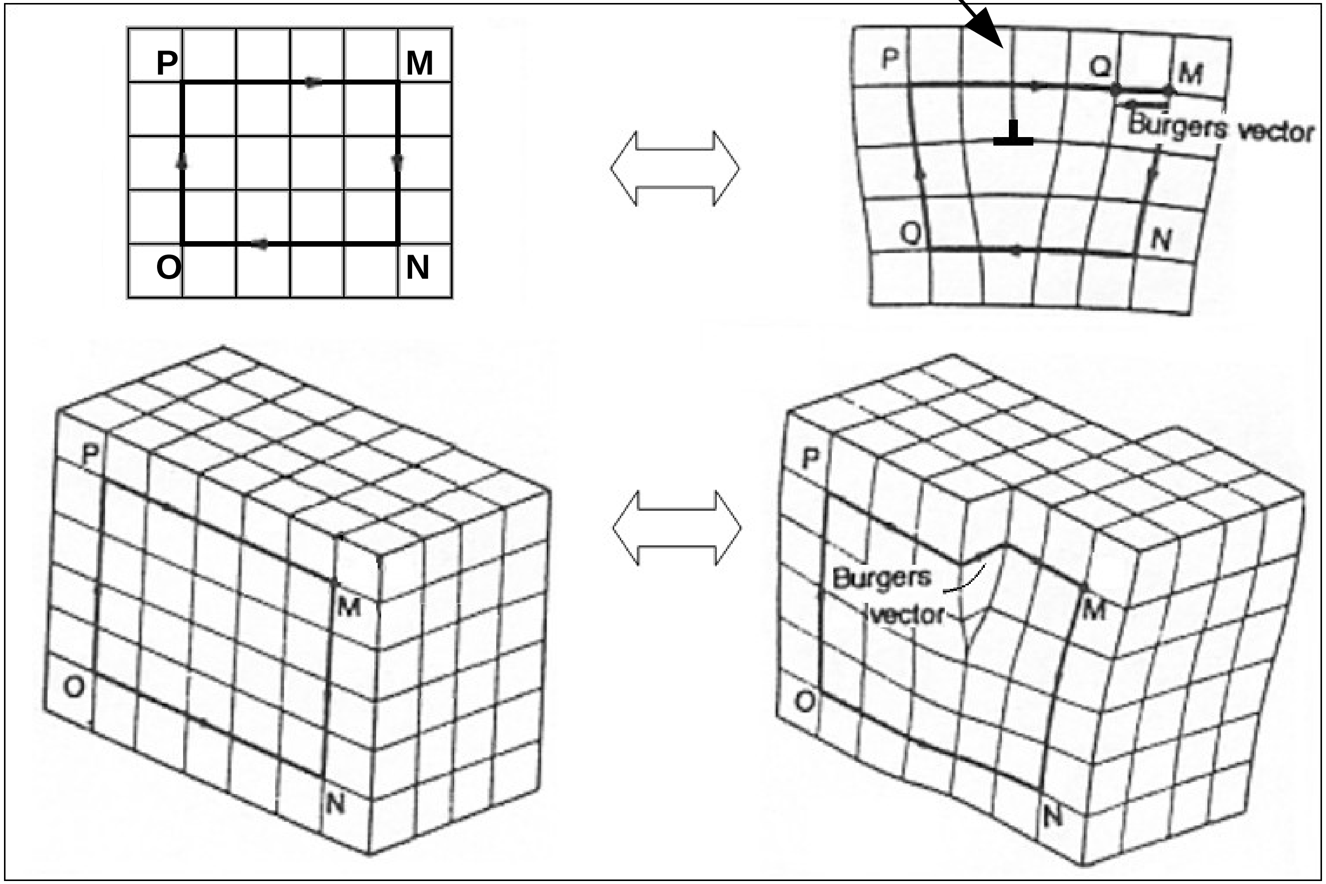

http://en.wikipedia.org/wiki/Dislocation

Dislocations in CVD Diamond

- **Basics**

  Classification by Burgers vector **b** and dislocation line direction **l**

Determination of Burgers vector **b** of an edge dislocation

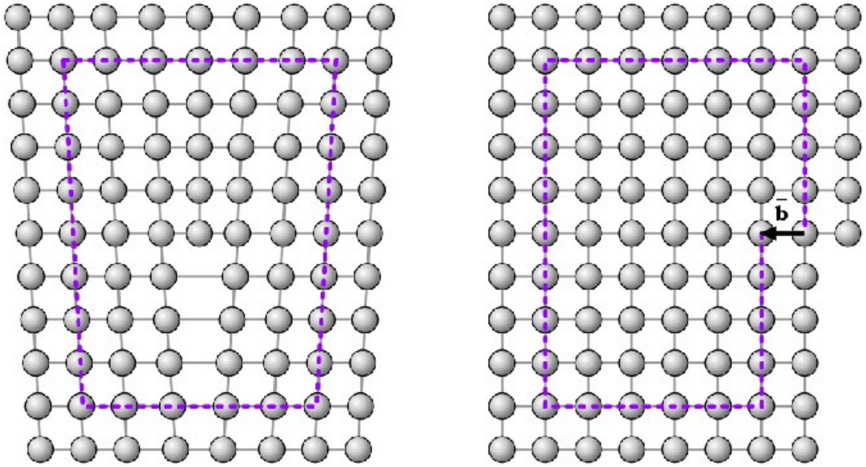

http://de.wikipedia.org/wiki/Versetzung_(Materialwissenschaft)

Dislocation line **l** (blue) of an edge dislocation

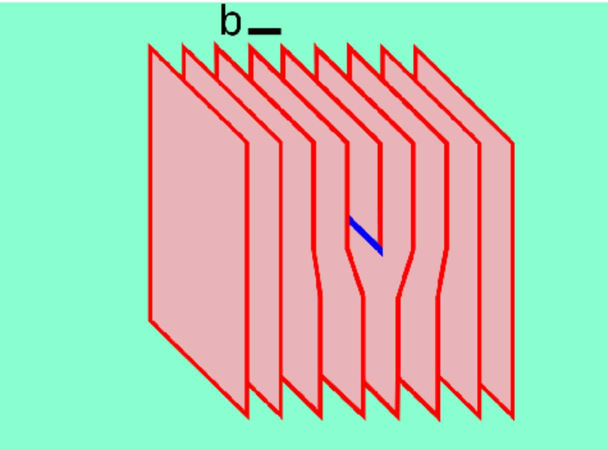

http://en.wikipedia.org/wiki/Dislocation

Edge dislocation:	**b** $\perp$ **l**
Screw dislocation:	**b** $\|\|$ **l**
Mixed dislocation:	else

Dislocations in CVD Diamond

- **Simplest types of dislocations in diamond**

Perfect dislocations of the {111}⟨110⟩ slip system

→ Screw dislocation, e.g. $\mathbf{l}_s$ = [1 -1 0], $\mathbf{b}_s$ = 1/2 [1 -1 0]

→ 60° dislocation, e.g. $\mathbf{l}_{60}$ = [1 -1 0], $\mathbf{b}_{60}$ = 1/2 [0 -1 1]

→ Edge dislocation, e.g. $\mathbf{l}_e$ = [-1 -1 2], $\mathbf{b}_e$ = 1/2 [-1 1 0]

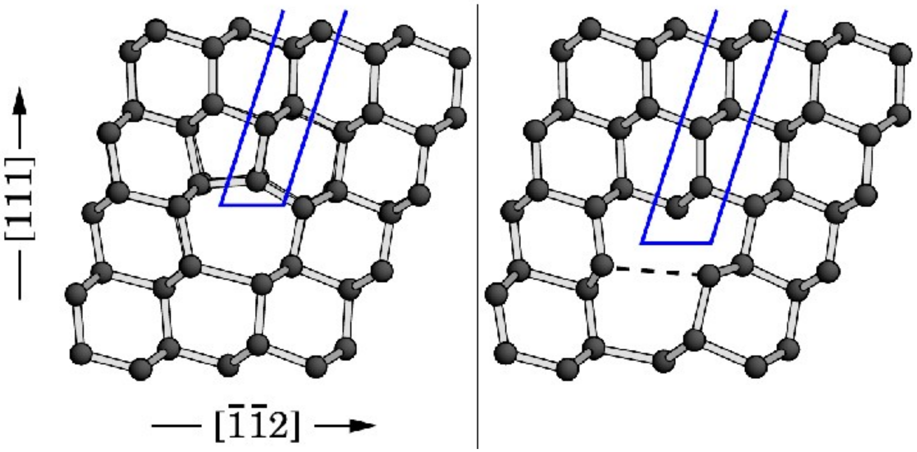

60° dislocation in diamond

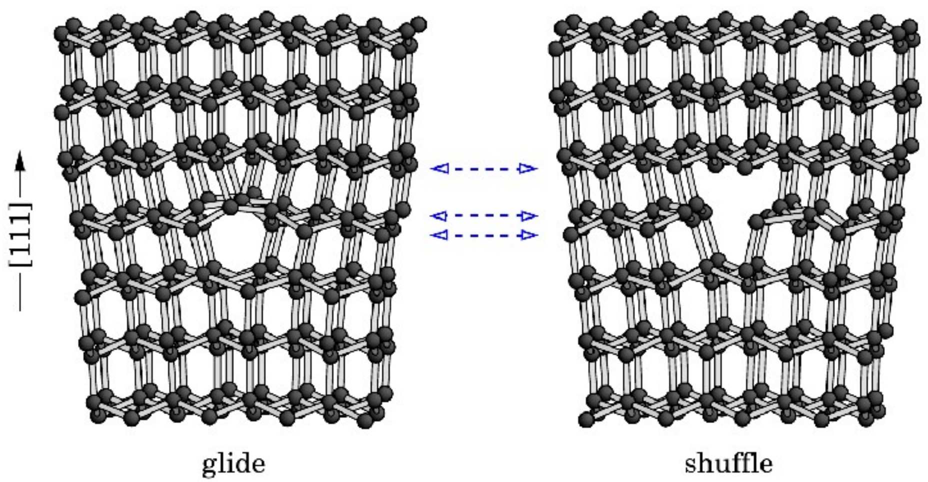

Perfect edge dislocation in diamond ($\mathbf{l}_e$ = [-1 -1 2])

This is only the tip of the iceberg!

A. Blumenau et al., Defects and Diffusion Forum 226-228 (2004) 11

Dislocations in CVD Diamond

- **Threading dislocations**

  Consequence of growth mechanism of heteroepitaxial diamond films
  → Generation of defect bands composed of small angle grain boundaries

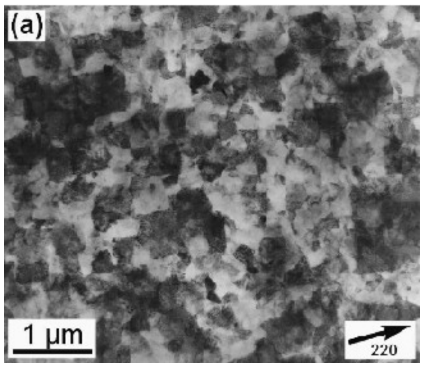

Film thickness 0.6 µm, grain size 0.3 µm

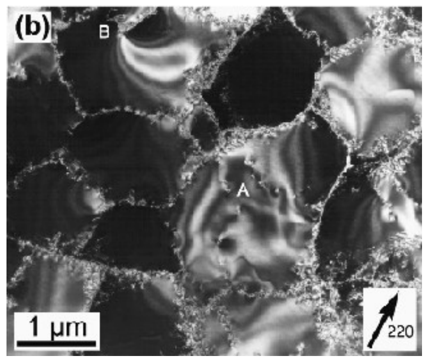

Film thickness 8 µm, grain size 1 µm

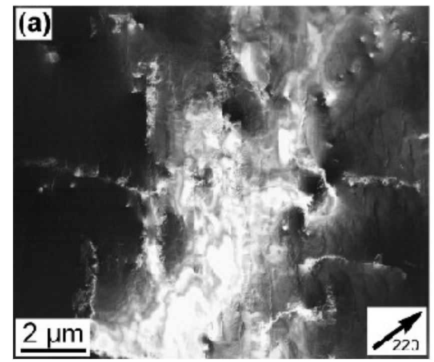

Film thickness 34 µm, no well-defined grains

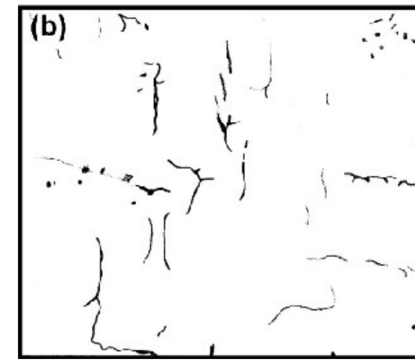

Film thickness 34 µm, defect bands highlighted

Plan view TEM images of thin heteroepitaxial CVD diamond films

→ Dislocation lines penetrating the whole diamond film nearly parallel to the growth direction

→ Initially very high dislocation density, comparable to nucleation density (10^{11} cm^{-2}), decreasing with film thickness

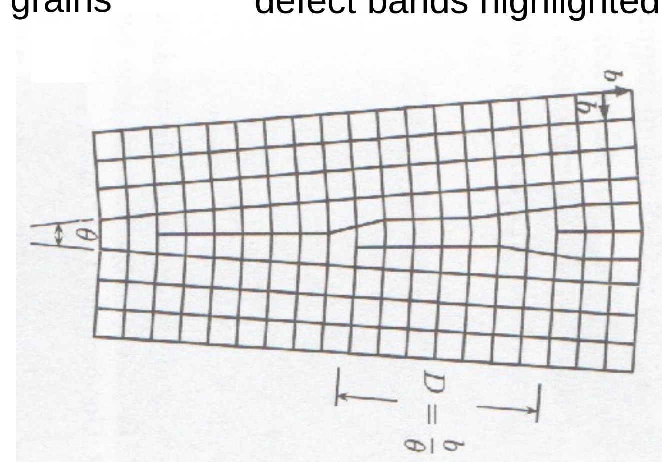

Edge dislocations forming a small angle grain boundary (top view)

C. Kittel: Einführung in die Festkörperphysik, 14th ed. (2006)

- **Common methods**

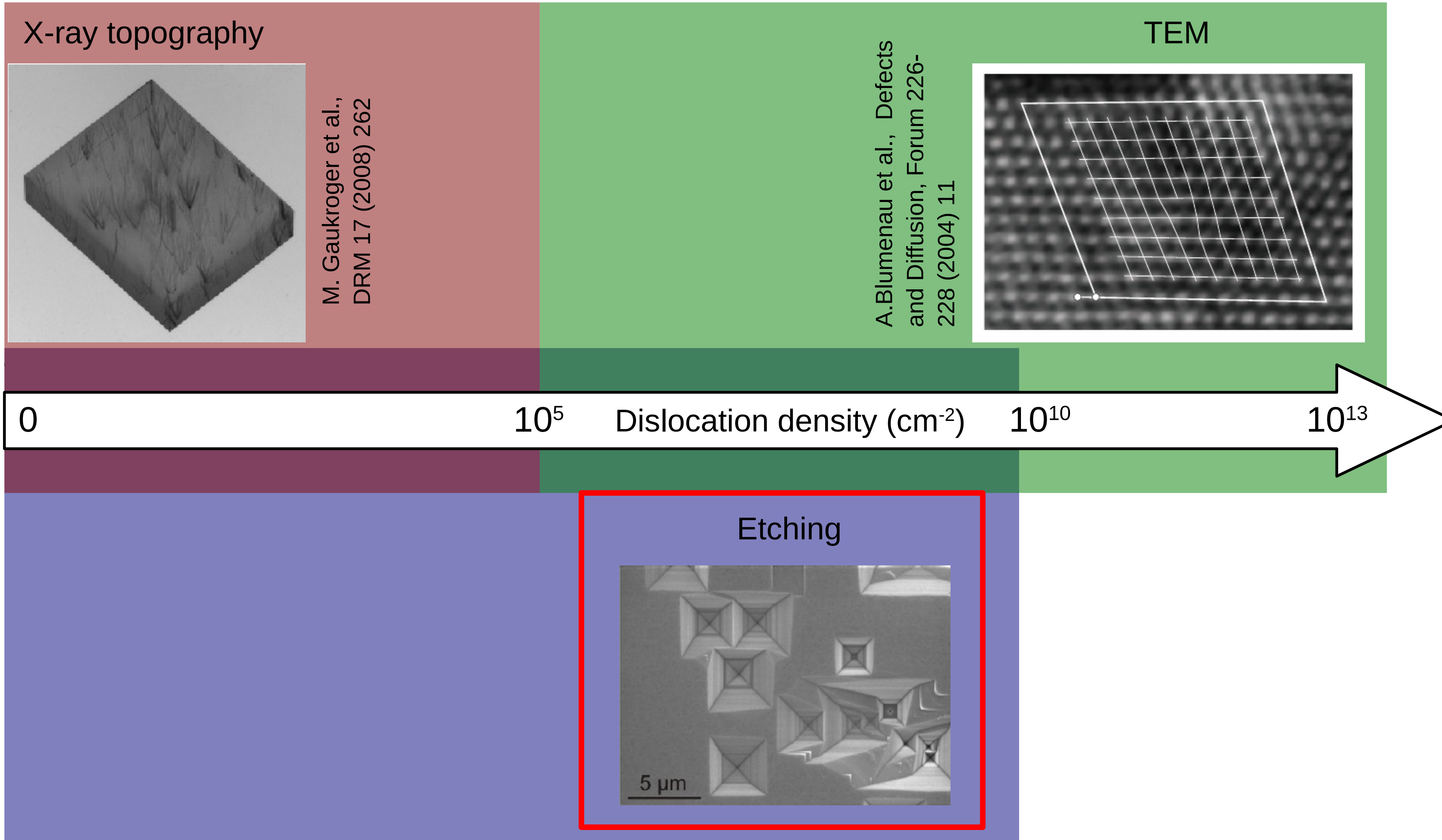

Values taken from K. Sangwal: Etching of Crystals (1987)

Detection of Dislocations

- **Etching**

  Plasma etching of diamond
  → Similar to CVD growth process
  → Addition of CO_2 instead of CH_4 in the gas phase
  → Formation of **etch-pits** at intersection of surface and dislocation line

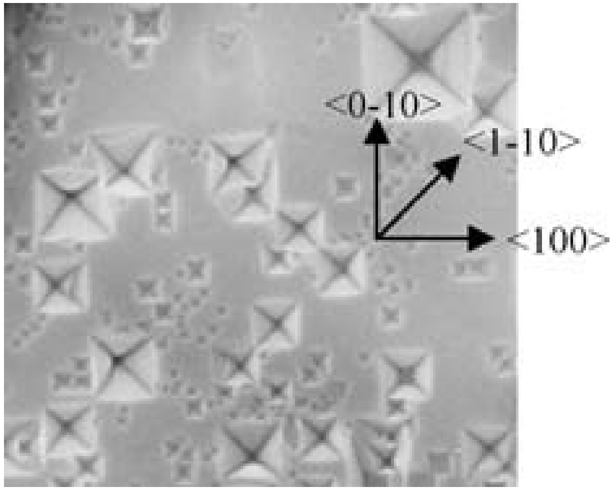

SEM image of etch-pits in diamond

J. Achard et al., PSS(A) 206 (2009) 1949

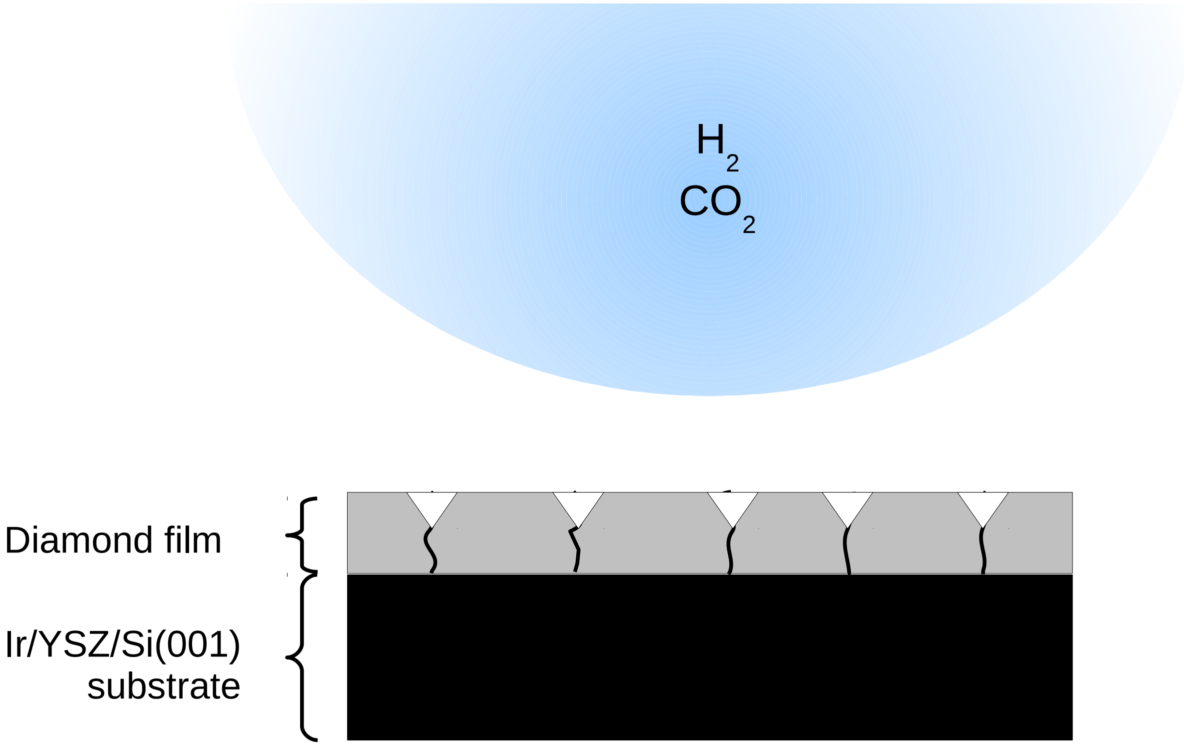

Advantages:

→ Compatible with existing CVD reactors
→ Fast
→ **Suitable for wide range of dislocation densities**

Detection of Dislocations

- **Experimental observations on DoI films**

  Etch pit distribution on “low-quality” crystals for neutron monochromators

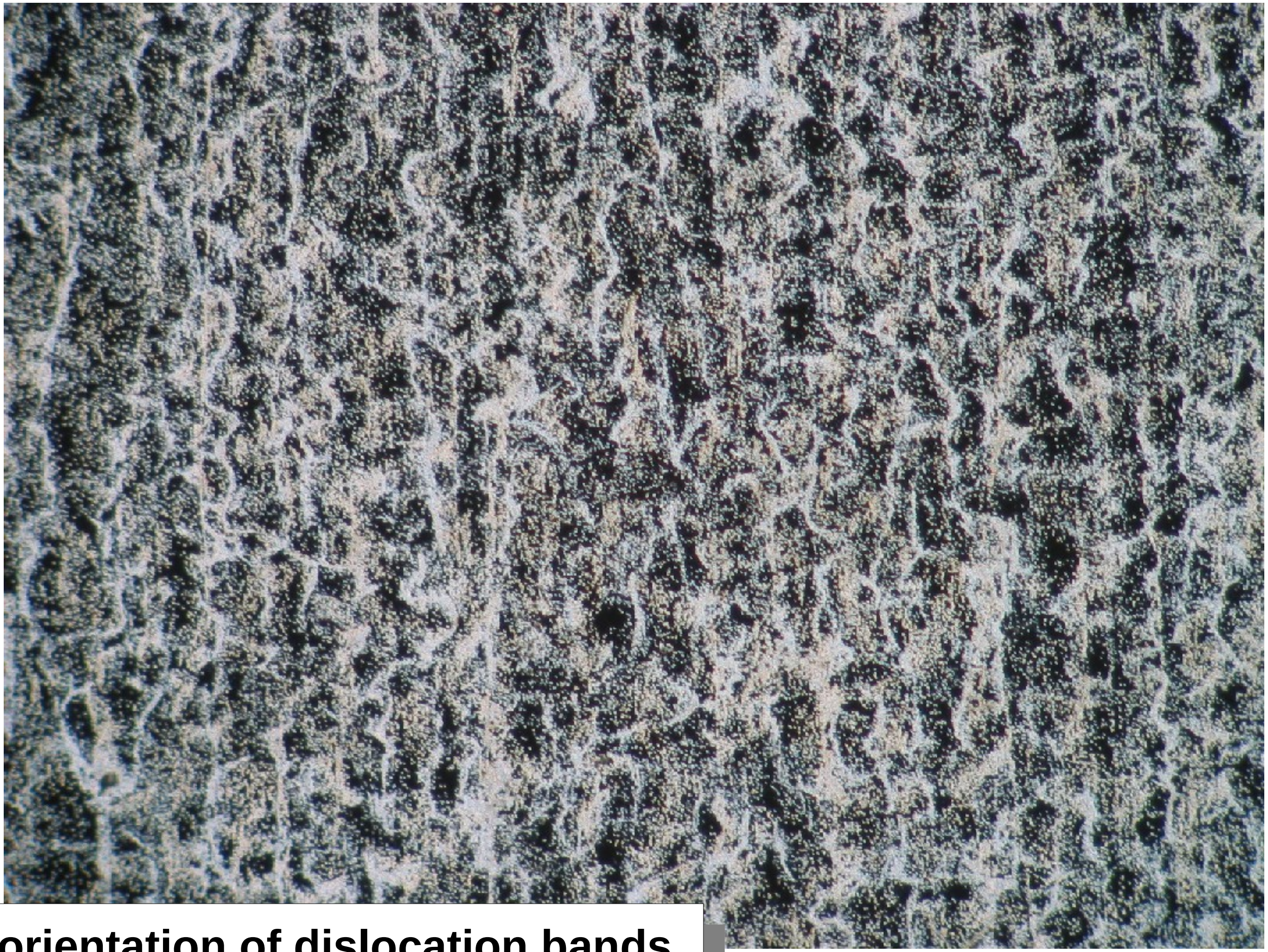

Preferential orientation of dislocation bands

Dark-field optical microscope image

Detection of Dislocations

- **Experimental observations on DoI films**

  Etch pit distribution on “low-quality” crystals for neutron monochromators

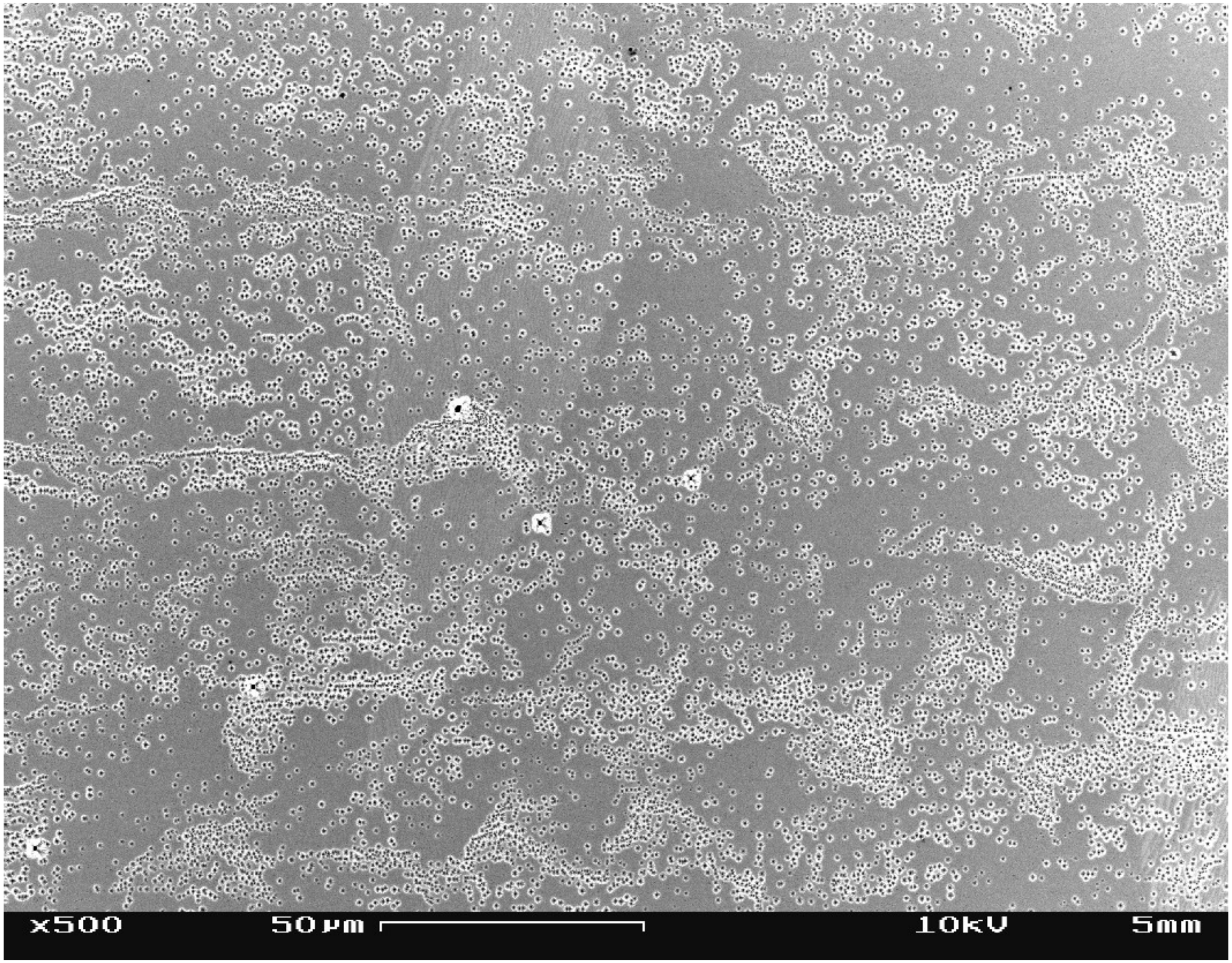

SEM image

Detection of Dislocations

- **Experimental observations on DoI films**

  Etch pit distribution on “low-quality” crystals for neutron monochromators

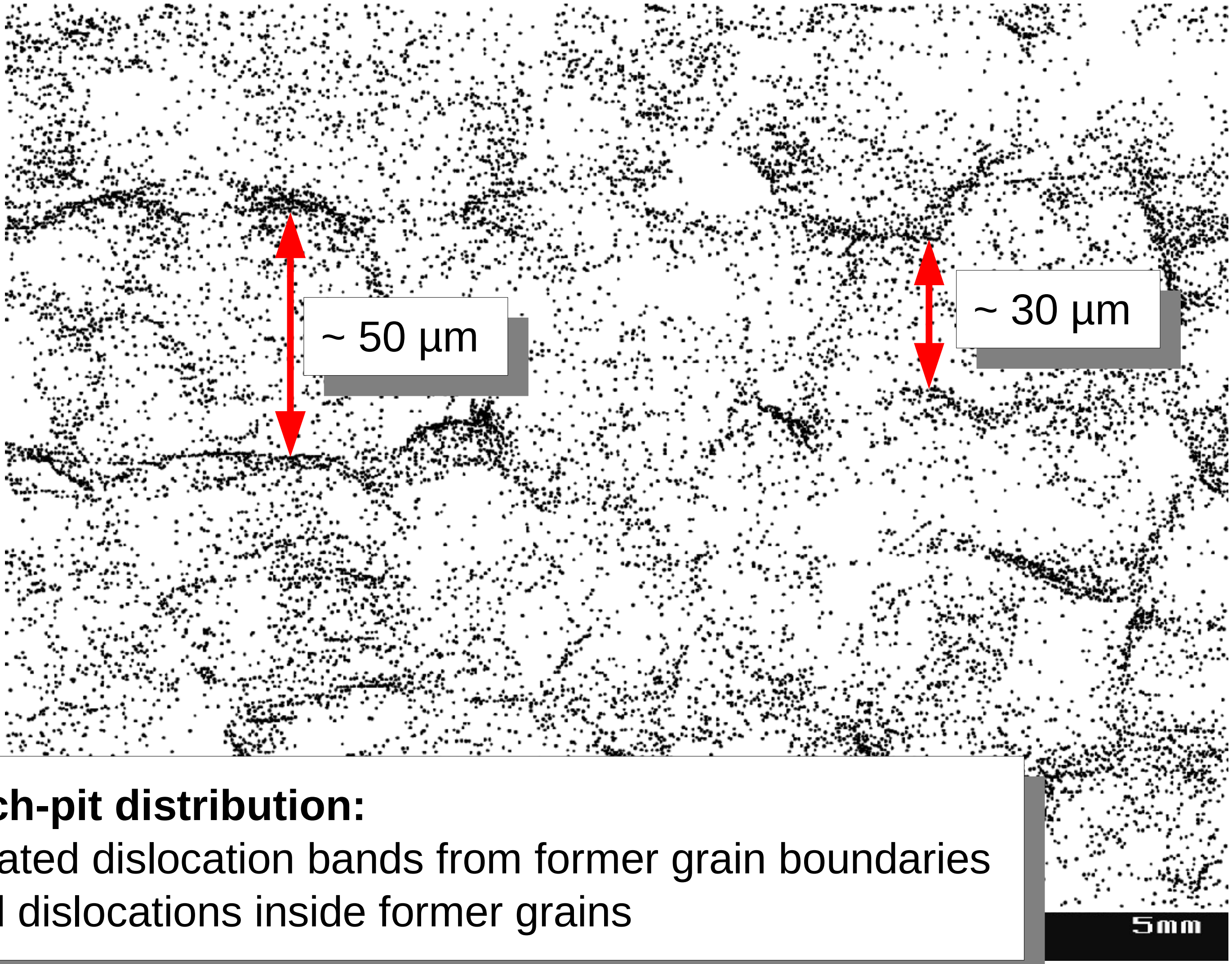

Bi-modal etch-pit distribution:
→ Agglomerated dislocation bands from former grain boundaries
→ Dispersed dislocations inside former grains

Extracted etch-pit positions

Detection of Dislocations

- **Experimental observations on DoI films**

  Photoluminescence pattern on “high-quality” crystal for detectors
  → **Blue luminescence correlated with dislocations**

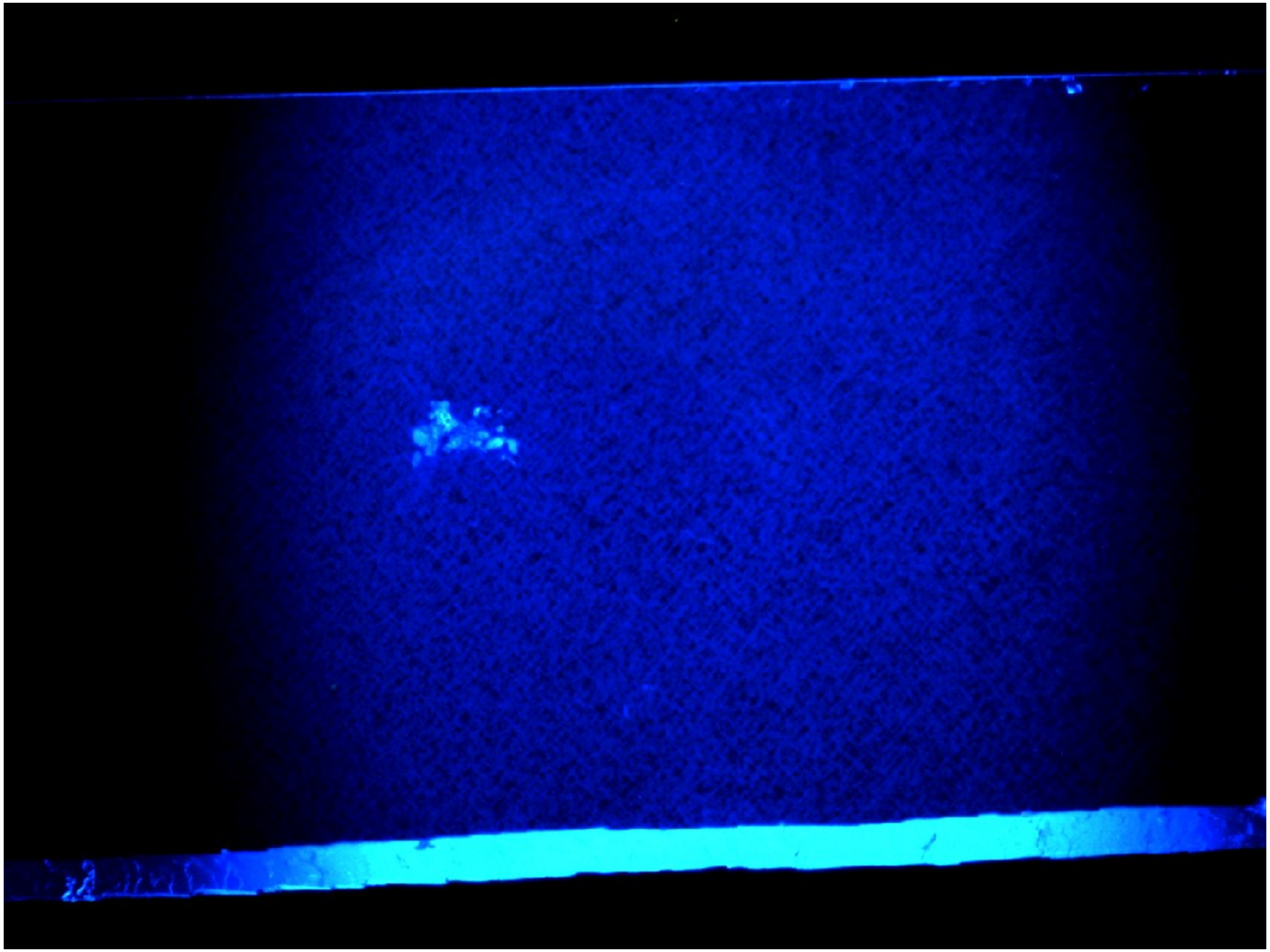

DiamondView image (UV excitation), courtesy of J. Achard

Detection of Dislocations

- **Experimental observations on DoI films**

  Photoluminescence pattern on “high-quality” crystal for detectors
  → **Blue luminescence correlated with dislocations**

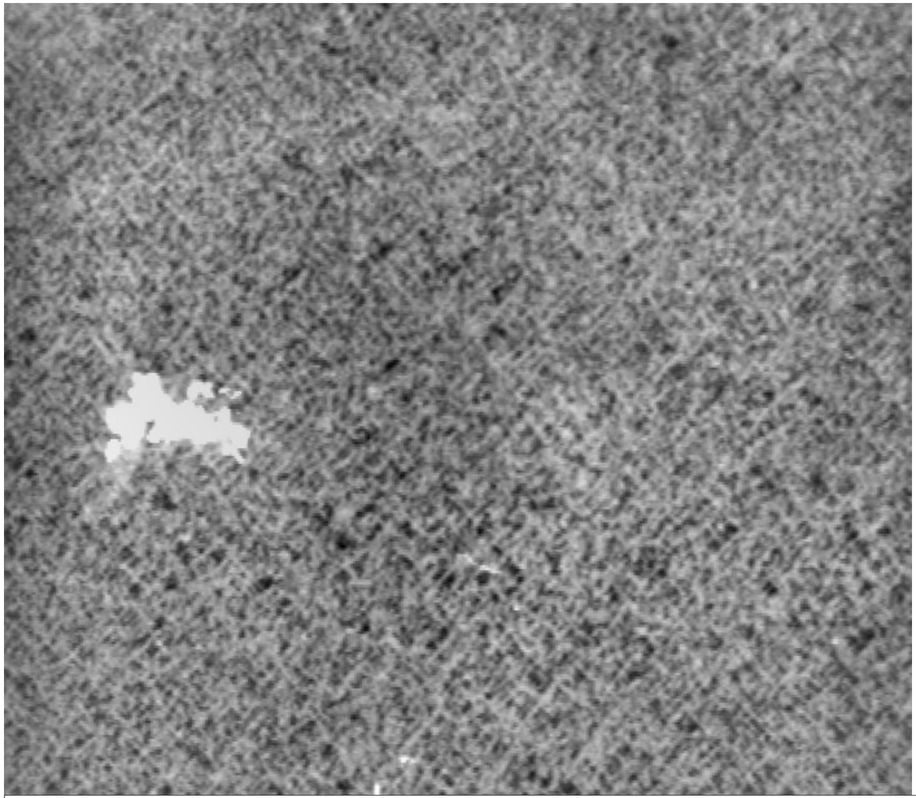

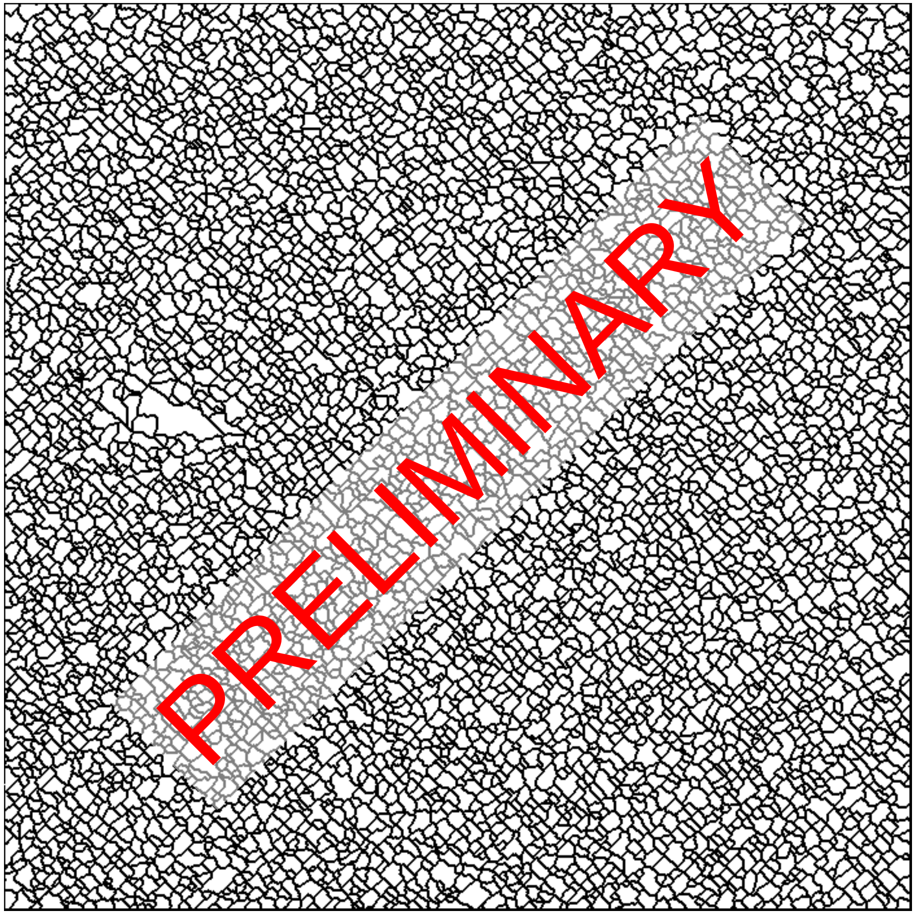

Luminescence bands automatically extracted by Watershed Algorithm
→ characteristic **length scale ~ 35 μm**

Detection of Dislocations

- **Experimental observations on DoI films**

  Unexpected similarity between "low-quality" monochromator crystals and "high-quality" detector crystals!

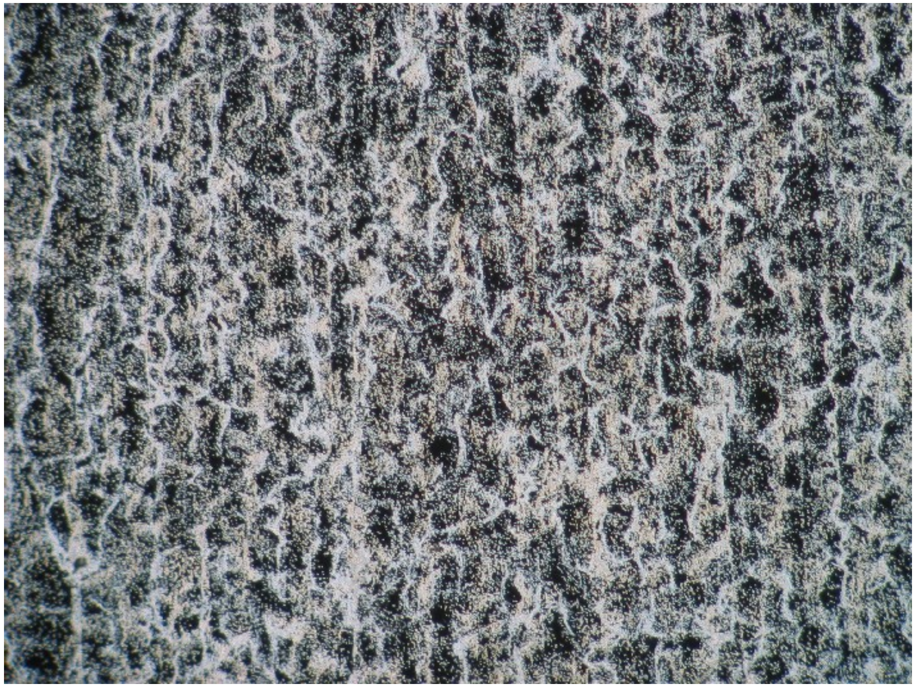

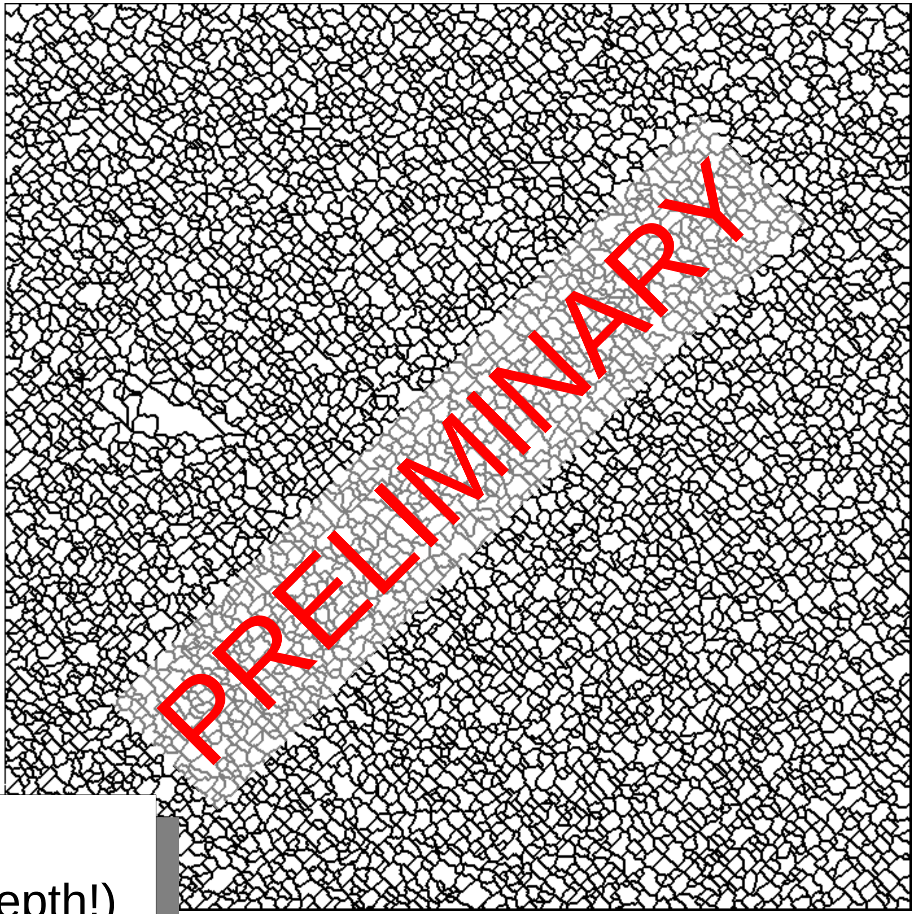

Further investigation necessary
→ Cathodoluminescence imaging (information depth!)
→ Thickness dependent etch-pit distribution

Reduction of Dislocation Density

- **Growth of thick layers**

A. Romanov et al., PSS(B) 198 (1996) 599

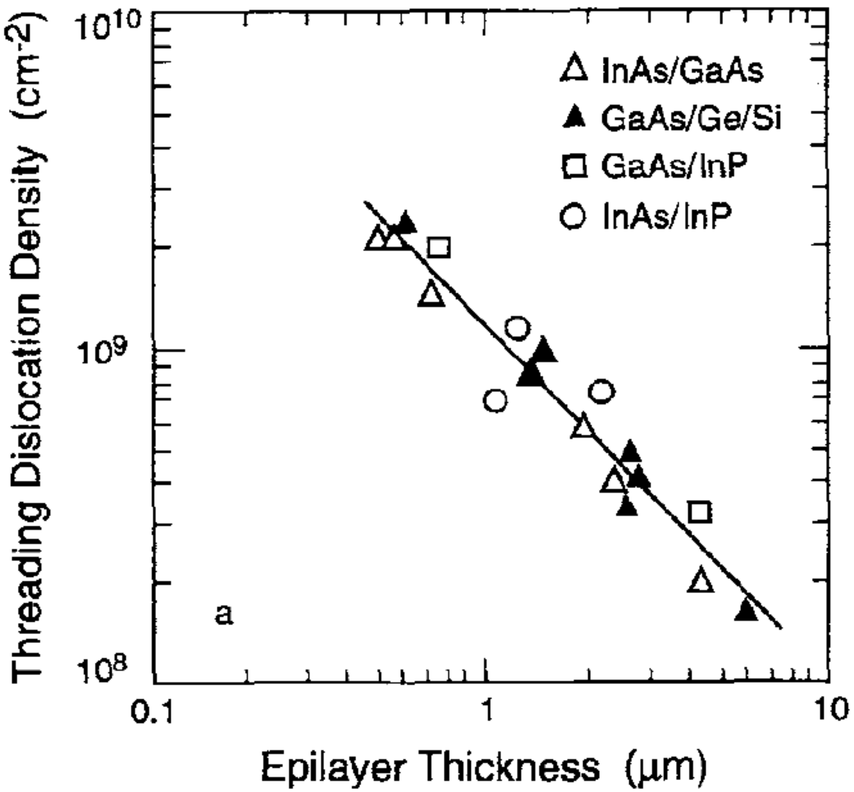

Dislocation density vs. film thickness for different heteroepitaxial material systems

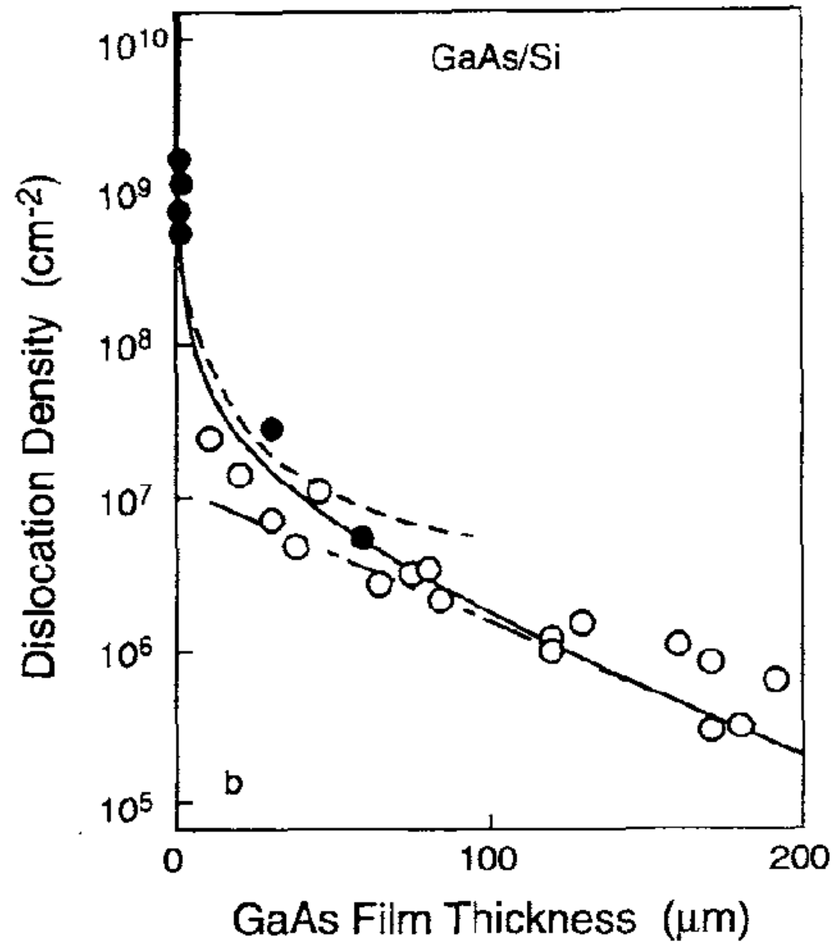

→ Common **1/d dependence** observed for other material systems

Reduction of Dislocation Density

- **Growth of thick layers**

  Descriptive explanation:
  Interaction of inclined dislocations during growth
  → Annihilation of dislocations with opposite Burgers vectors

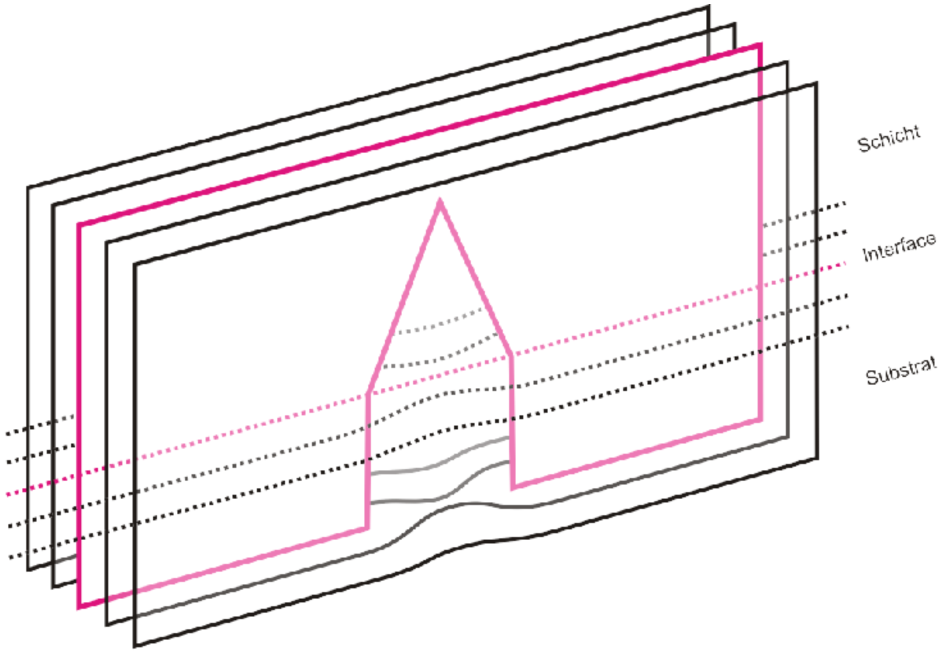

Top-view

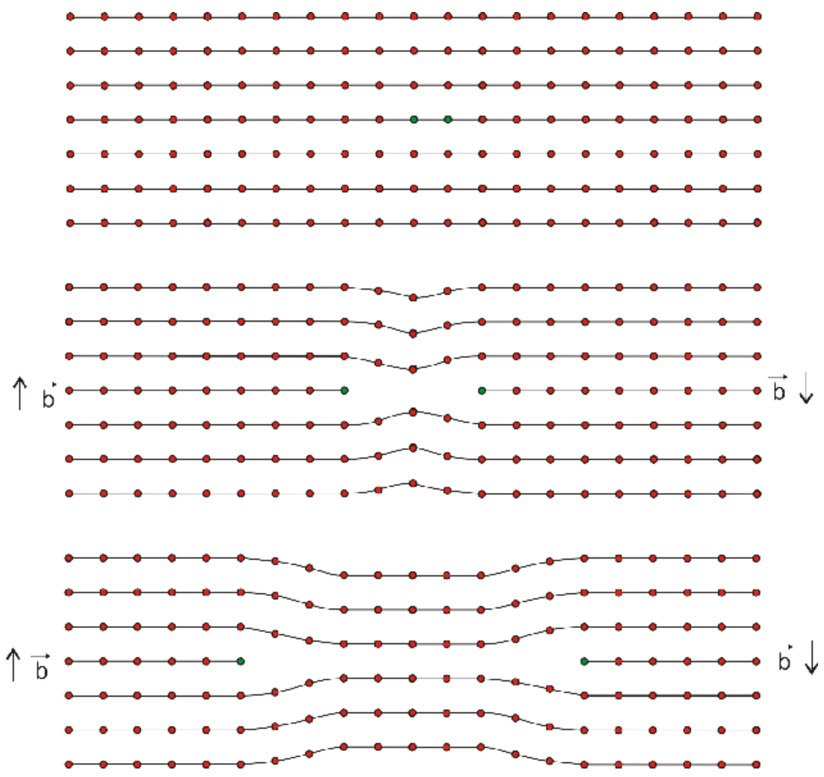

> → **Reduction of dislocation density by growth of thick layers possible**

Reduction of Dislocation Density

- **Growth of thick layers**

  Descriptive explanation:
  Interaction of inclined dislocations during growth
  → Annihilation of dislocations with opposite Burgers vectors

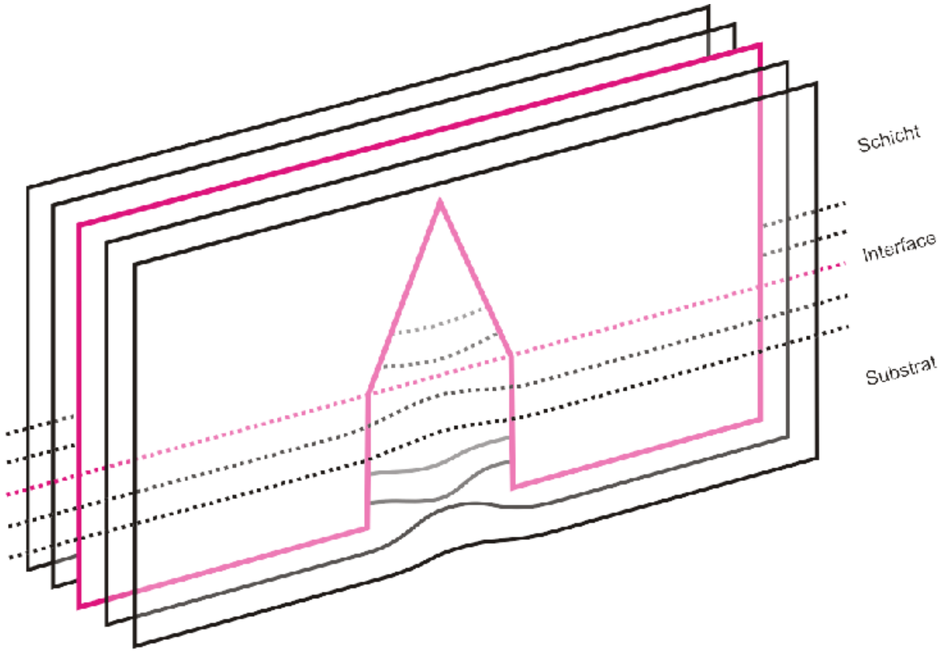

Top-view

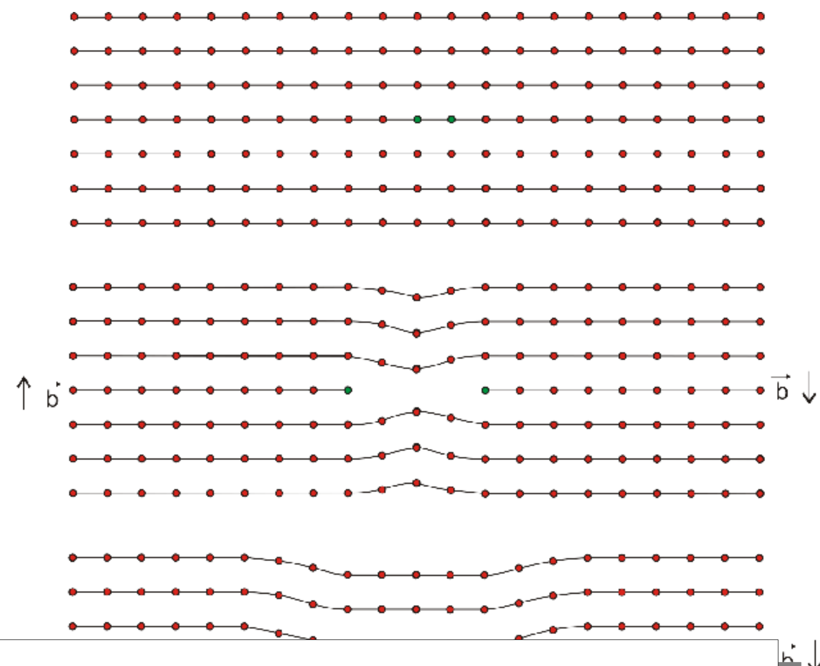

→ **Reduction of dislocation density by growth of thick layers possible**

→ **Mathematical modelling yields experimental 1/d dependence**

Reduction of Dislocation Density

- **Experimental observations on DoI films**

  Etch pit density on films of different thickness

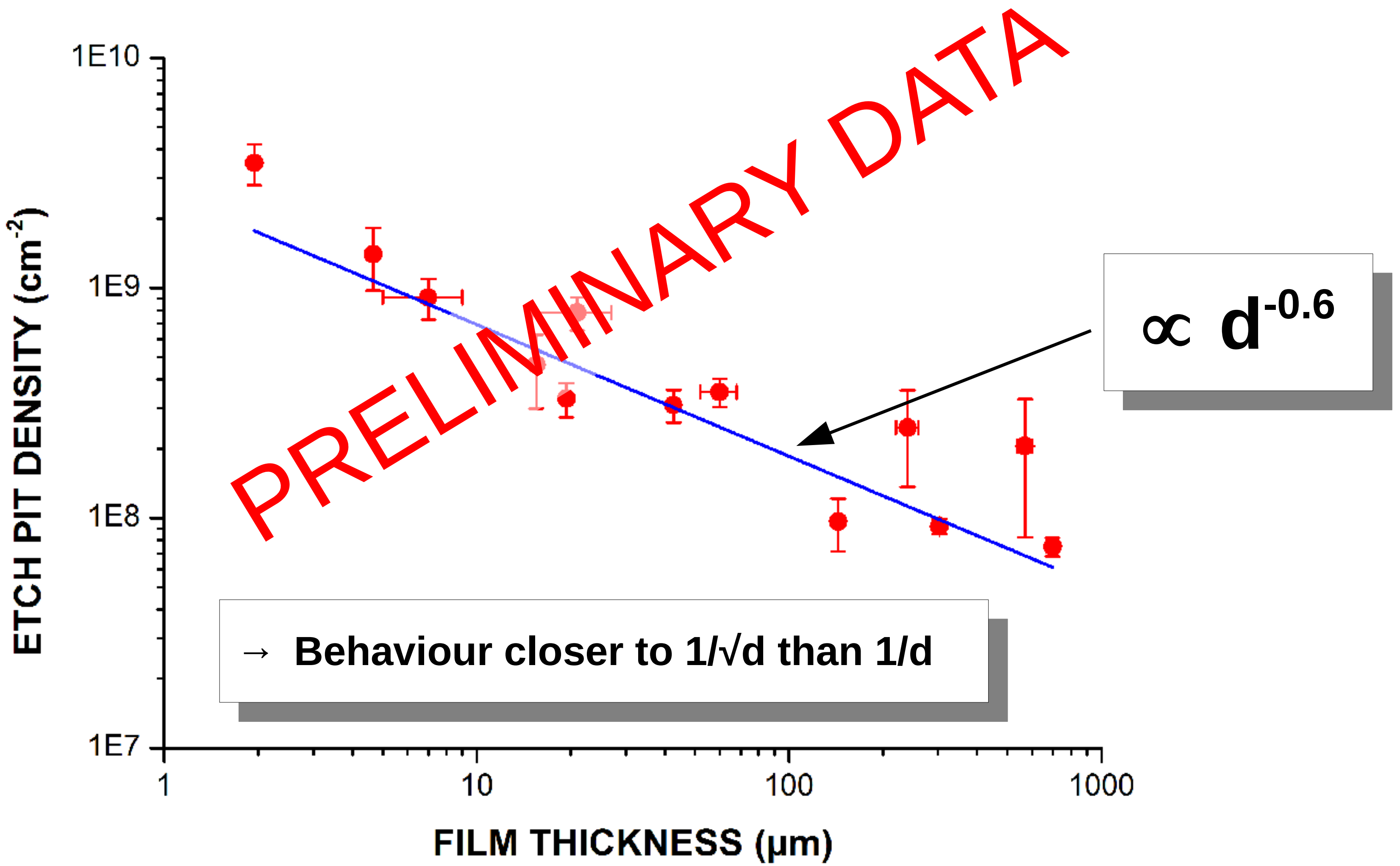

Reduction of Dislocation Density

- **Experimental observations on DoI films**

  Etch pit density on films of different thickness

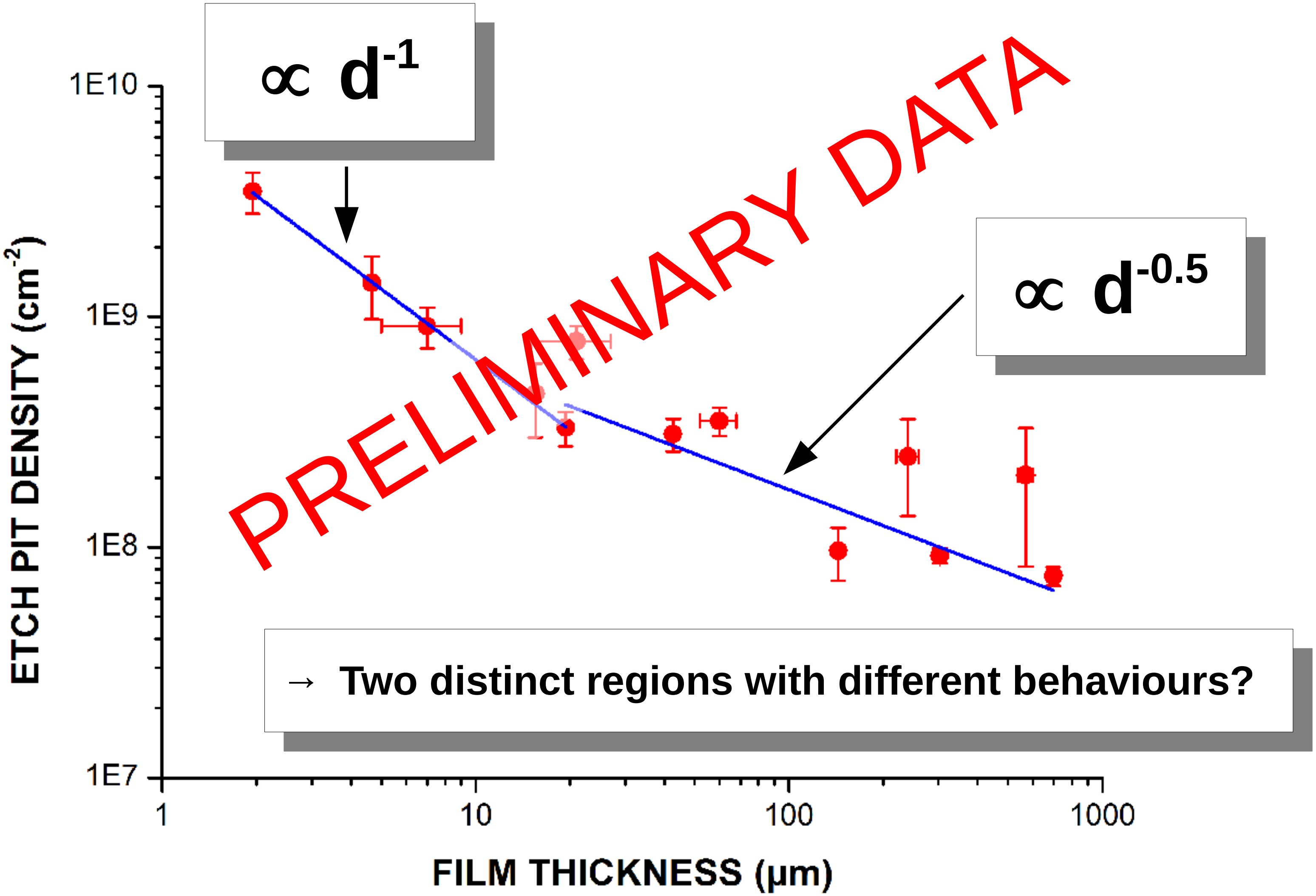

- **Dislocation density spectrum of diamond materials**

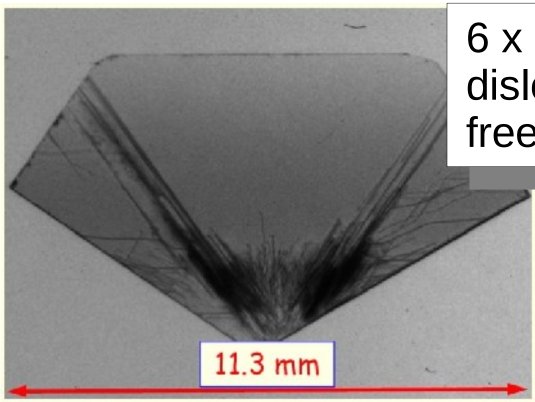

6 x 4 mm^2
dislocation
free area

Y. Shvyd'ko et al., Nature Photonics **5**, 539 (2011)

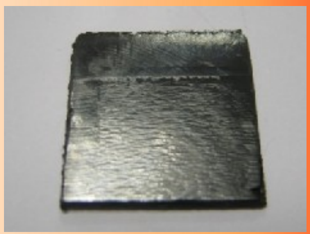

Diamond on Iridium

0 Dislocation density (cm^{-2}) 10^4 10^6 10^8 10^9 10^{11}

Single crystal CVD diamond

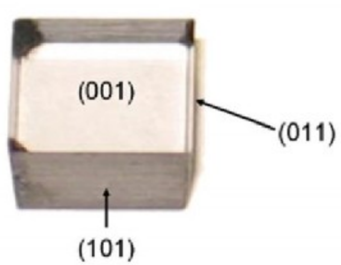

Single crystal HPHT diamond

Natural IIa,
brown - colourless

R.S. Balmer et al.: *Chemical vapour deposition synthetic diamond: material, technology and applications* J. Phys.: Condens. Matter 21 (2009) 364221

Further investigations

- TEM measurements
  → Dislocation type
  → Dislocation line direction
- Creating larger etch-pit data set
  → Spatial etch-pit distribution at different growth stages
  → Dislocation density reduction and modelling of thickness dependence
- Correlation of etch-pits and Raman/luminescence measurements
- Investigation of etch-pit morphology
- **Correlation with detector performance**

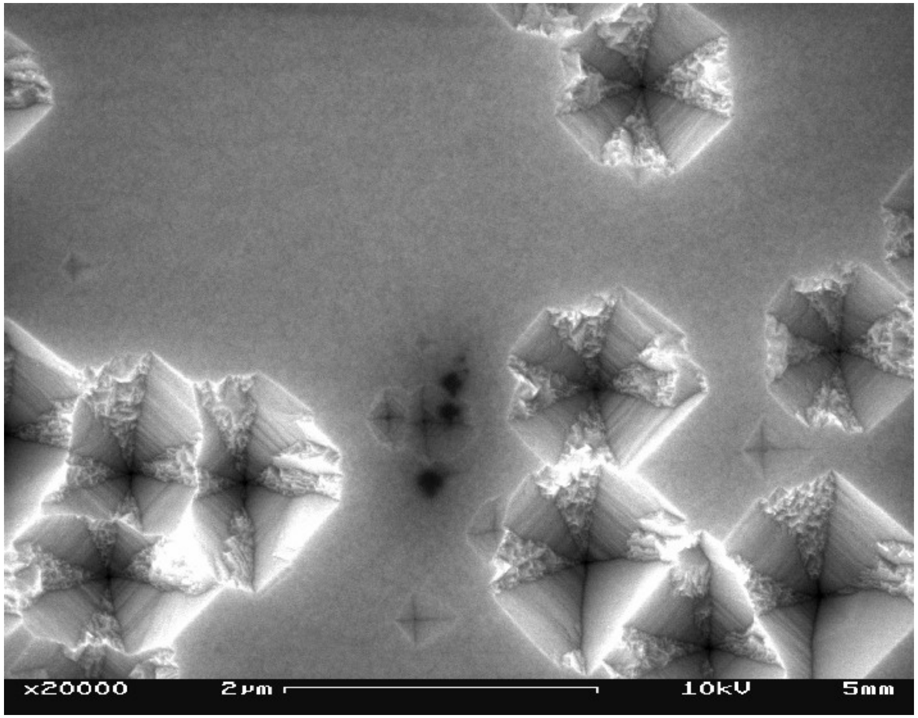

Etch-pits of different size and shape

Acknowledgements

- GSI
  - E. Berdermann
  - C. Schmidt
  - M. Träger
- Centre National de la Recherche Scientifique
  - J. Achard
- Universität Augsburg
  - S. Gsell
  - A. Sartori
  - M. Weinl
- Funding by the EC